Inorganic Chemistry

Novel Tailoring Reaction for Two Adjacent Coordinated Nitriles Giving Platinum 1,3,5-Triazapentadiene Complexes

Pavel V. Gushchin,[†] Marina R. Tyan,[†] Nadezhda A. Bokach,[†] Mikhail D. Revenco,[‡] Matti Haukka,[§] Meng-Jiy Wang,[⊥] Cheng-Hsuan Lai,[¶] Pi-Tai Chou,*[¶] and Vadim Yu. Kukushkin*[†,‖]

St. Petersburg State University, 198504 Stary Petergof, Russian Federation, Department of Chemistry, State University of Moldova, MD 2009 Chisinau, Republic of Moldova, Institute of Macromolecular Compounds of the Russian Academy of Sciences, Bolshoii Pr. 31, 199004 St. Petersburg, Russian Federation, Department of Chemistry, University of Joensuu, P.O. Box 111, FI-80101 Joensuu, Finland, Department of Chemical Engineering, National Taiwan University of Science and Technology, 43, Keelung Road, Section 4, Taipei, 106 Taiwan, and Department of Chemistry, National Taiwan University, No. 1, Roosevelt Road, Section 4, Taipei, Taiwan

The tailoring reaction of the two adjacent nitrile ligands in *cis*-[PtCl$_2$(RCN)$_2$] (R = Me, Et, CH$_2$Ph, Ph) and [Pt(tmeda)(EtCN)$_2$][SO$_3$CF$_3$]$_2$ (**8**·(OTf)$_2$; tmeda = *N,N,N′,N′*-tetramethylethylenediamine) upon their interplay with *N,N′*-diphenylguanidine (DPG; NH=C(NHPh)$_2$), in a 1:2 molar ratio gives the 1,3,5-triazapentadiene complexes [PtCl$_2${*N*HC(R)NHC(R)=*N*H}] (**1**–**4**) and [Pt(tmeda){*N*HC(Et)NHC(Et)*N*H}][SO$_3$CF$_3$]$_2$ (**10**·(OTf)$_2$), respectively. In contrast to the reaction of **8**·(OTf)$_2$ with NH=C(NHPh)$_2$, interaction of **8**·(OTf)$_2$ with excess gaseous NH$_3$ leads to formation of the platinum(II) bis(amidine) complex *cis*-[Pt(tmeda){NH=C(NH$_2$)Et}$_2$][SO$_3$CF$_3$]$_2$ (**9**·(OTf)$_2$). Treatment of *trans*-[PtCl$_2$(RCN)$_2$] (R = Et, CH$_2$Ph, Ph) with 2 equiv of NH=C(NHPh)$_2$ in EtCN (R = Et) and CH$_2$Cl$_2$ (R = CH$_2$Ph, Ph) solutions at 20–25 °C leads to [PtCl{*N*H=C(R)NC(NHPh)=*N*Ph}(RCN)] (**11**–**13**). When any of the *trans*-[PtCl$_2$(RCN)$_2$] (R = Et, CH$_2$Ph, Ph) complexes reacts in the corresponding nitrile RCN with 4 equiv of DPG at prolonged reaction time (75 °C, 1–2 days), complexes containing two bidentate 1,3,5-triazapentadiene ligands, i.e. [Pt{*N*H=C(R)NC(NHPh)=*N*Ph}$_2$] (**14**–**16**), are formed. Complexes **14**–**16** exhibit strong phosphorescence in the solid state, with quantum yields (peak wavelengths) of 0.39 (530 nm), 0.61 (460 nm), and 0.74 (530 nm), respectively. The formulation of the obtained complexes was supported by satisfactory C, H, and N elemental analyses, in agreement with FAB-MS, ESI-MS, IR, and ^{1}H and ^{13}C{^{1}H} NMR spectra. The structures of **1**, **2**, **4**, **11**, **13**, **14**, **9**·(picrate)$_2$, and **10**·(picrate)$_2$ were determined by single-crystal X-ray diffraction.

Introduction

1,3-Dicarbonyl derivatives (Chart 1, **A**) in general and acetylacetone in particular represent one of the oldest and, concurrently, one of the most valuable classes of ligands for metal ion chelation with a substantial fraction of the elements in the periodic table. The rich chemistry of these species is well-documented, and a good number of industrial applica-

tions are known.[1] The *dinitrogen* analogues of 1,3-dicarbonyl compounds, i.e. 1,5-diazapentadienyl (or *β*-diketiminate) species (**B**), have been much less studied but over the past decade they have fast become one of the most useful groups of monoanionic nitrogen-based ligands in chemistry. Their complexes serve as useful models for synthetic, reactivity, and structural investigations[2–5] and also for modeling active sites of metalloenzymes.[6] In addition, *β*-diketiminates of

* Author to whom correspondence should be addressed. E-mail: kukushkin@vk2100.spb.edu.

† St. Petersburg State University.

‖ Institute of Macromolecular Compounds of the Russian Academy of Sciences.

‡ State University of Moldova.

§ University of Joensuu.

⊥ National Taiwan University of Science and Technology.

¶ National Taiwan University.

(1) Pettinari, C.; Marchetti, F.; Drozdov, A. *β*-Diketones and Related Ligands. In *Comprehensive Coordination Chemistry*, 2nd ed.; Elsevier: Amsterdam, 2004; Vol. 1, Chapter 1.6, pp 97–115.

(2) (a) Piers, W.; Emslie, D. J. H. *Coord. Chem. Rev.* **2002**, *131*, 233. (b) Bailey, P. J.; Pace, S. *Coord. Chem. Rev.* **2001**, *214*, 91. (c) Coles, M. P. *Dalton Trans.* **2006**, 985.

(3) Bourget-Merle, L.; Lappert, M. F.; Severn, J. R. *Chem. Rev.* **2002**, *102*, 3031.

Chart 1. Skeletons of 1,3-Dicarbonyl (**A**), 1,5-Diazapentadienyl (**B**), and 1,3,5-Triazapentadienyl (**C**) Species
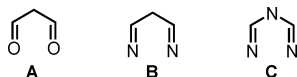
labile metal centers have intrinsic practical applications: e.g., as polymerization catalysts.[7–9]

The *trinitrogen* analogues of the 1,3-dicarbonyls, i.e. 1,3,5-triazapentadienyl (or imidoylamidine) species (**C**), have been substantially less explored than the relevant **A** and **B** systems, but they deserve special attention from coordination chemists, as **C** ligands offer an additional coordination site at the central nitrogen atom, especially in their anionic form. Moreover, this N atom takes part in facile acid–base equilibria,[10–12] thus providing pH sensing properties to their complexes: e.g., those exhibiting luminescent properties.[12] Despite the obvious advantages and potential of the 1,3,5-triazapentadienyl chelating systems, these species are small in number, since as facile and general synthetic methods for their generation have thus far been rather poorly developed.

Thus, reactions between the *pre*prepared 1,3,5-triazapentadiene and metal sources are rather rare because the ligands, especially those with donor substituents, are highly reactive and therefore many of them are *elusive* in the free state. Direct metal–ligand reactions have been realized only with stable 1,3,5-triazapentadienes, which bear strong electron acceptor groups at the C atoms, e.g. fluoroalkyls, and they are N substituted, e.g. NAr.[13–18]

The unstable 1,3,5-triazapentadienes, which are unsubstituted at the NH groups and/or contain donor substituents at the carbon atoms (**C**), are typically prepared by metal-mediated reactions such as (i) coupling between amidine(ate)s and nitriles electrophilically activated by ligation to M^{II} (Pt^{II},[12,19,20] Pd^{II},[19,21] Ni^{II} [22]) and Pt^{IV} [20] centers, (ii) cop-

per-[23,24] or nickel-mediated[25] hydrolytic conversion of 1,3,5-triazine[23,25] or 1,3,5-tris(2-pyridyl)-2,4,6-triazine,[24] (iii) hydrolytic conversion of RCN mediated by the dinuclear nickel(II) complex $[Ni_2(\mu\text{-}OH)_2(tpa)_2](ClO_4)_2$ (tpa = tris-(2-pyridylmethyl)amine)[26] or Ni(II) acetate,[27] (iv) evaporating a MeOH solution of $NiCl_2 \cdot 6H_2O$ and acetamidine,[28] and (v) by oxime-assisted conversion of nitriles at Pt^{II} [29] and Ni^{II} [10,11] centers.

In the course of our ongoing studies on reactions of metal-activated nitriles,[30] giving in particular 1,3,5-triazapentadiene complexes,[10–12,20] we have discovered a novel tailoring reaction between the guanidine $NH=C(NHPh)_2$ (DPG) and two cis nitriles at the Pt^{II} center, leading to platinum(II) 1,3,5-triazapentadiene complexes. The developed method, which is based on this reaction, represents a facile route to (1,3,5-triazapentadiene)Pt^{II} species with luminescent properties. Details of these results are elaborated in this article.

Results and Discussion

We have recently reported[31] on the coupling between tetramethylguanidine ($HN=C(NMe_2)_2$) and coordinated organonitriles in the platinum(II) complexes *cis-/trans*-$[PtCl_2(RCN)_2]$ (R = Me, Et, Ph), which proceeded rapidly

(4) Brown, E. C.; Bar-Nahum, I.; York, J. T.; Aboelella, N. W.; Tolman, W. B. *Inorg. Chem.* **2007**, *46*, 486. Tonzetich, Z. J.; Jiang, A. J.; Schrock, R. R.; Müller, P. *Organometallics* **2006**, *25*, 4725. Thompson, J. S.; Bradley, A. Z.; Park, K.-H.; Dobbs, K. D.; Marshall, W. *Organometallics* **2006**, *25*, 2712. Gherman, B. F.; Tolman, W. B.; Cramer, C. J. *J. Comput. Chem.* **2006**, *27*, 1950.

(5) York, J. T.; Llobet, A.; Cramer, C. J.; Tolman, W. B. *J. Am. Chem. Soc.* **2007**, *129*, 7990. Sadique, A. R.; Gregory, E. A.; Brennessel, W. W.; Holland, P. L. *J. Am. Chem. Soc.* **2007**, *129*, 8112. Ruspic, C.; Nembenna, S.; Hofmeister, A.; Magull, J.; Harder, S.; Roesky, H. W. *J. Am. Chem. Soc.* **2006**, *128*, 15000.

(6) Shimokawa, C.; Teraoka, J.; Tachi, Y.; Itoh, S. I. *Inorg. Biochem.* **2006**, *100*, 1118. Aboelella, N. W.; Gherman, B. F.; Hill, L. M. R.; York, J. T.; Holm, N.; Young, V. G.; Cramer, C. J.; Tolman, W. B. *J. Am. Chem. Soc.* **2006**, *128*, 3445. Cotton, S. A. *Annu. Rep. Prog. Chem., Sect. A: Inorg. Chem.* **2005**, *101*, 208.

(7) Li, Y.; Wang, L.; Gao, H.; Zhu, F.; Wu, Q. *Appl. Organomet. Chem.* **2006**, *20*, 436. Smith, K. M. *Curr. Org. Chem.* **2006**, *10*, 955.

(8) Li, Y.; Jiang, L.; Wang, L.; Gao, H.; Zhu, F.; Wu, Q. *Appl. Organomet. Chem.* **2006**, *20*, 181. Yao, Y.; Zhang, Z.; Peng, H.; Zhang, Y.; Shen, Q.; Lin, J. *Inorg. Chem.* **2006**, *45*, 2175.

(9) Fabri, F.; Muterle, R. B.; de Oliveira, W.; Schuchardt, U. *Polymer* **2006**, *47*, 4544. Sánchez-Barba, L. F.; Hughes, D. L.; Humphrey, S. M.; Bochmann, M. *Organometallics* **2006**, *25*, 1012. Vitanova, D. V.; Hampel, F.; Hultzsch, K. C. *J. Organomet. Chem.* **2005**, *690*, 5182.

(10) Kopylovich, M. N.; Pombeiro, A. J. L.; Fischer, A.; Kloo, L.; Kukushkin, V. Yu. *Inorg. Chem.* **2003**, *42*, 7239.

(11) Kopylovich, M. N.; Haukka, M.; Kirillov, A. M.; Kukushkin, V. Yu.; Pombeiro, A. J. L. *Chem. Eur. J.* **2007**, *13*, 786.

(12) Sarova, G. H.; Bokach, N. A.; Fedorov, A. A.; Berberan-Santos, M. N.; Kukushkin, V. Yu.; Haukka, M.; Fraústo-da-Silva, J. J. R.; Pombeiro, A. J. L. *Dalton Trans.* **2006**, 3798.

(13) Dias, H. V. R.; Singh, S. *Dalton Trans* **2006**, 1995. Dias, H. V. R.; Singh, S. *Inorg. Chem.* **2004**, *43*, 7396. Dias, H. V. R.; Singh, S. *Inorg. Chem.* **2004**, *43*, 5786.

(14) Siedle, A. R.; Webb, R. J.; Brostrom, M.; Newmark, R. A.; Behr, F. E.; Young, V. G., Jr. *Organometallics* **2004**, *23*, 2281. Siedle, A. R.; Webb, R. J.; Behr, F. E.; Newmark, R. A.; Weil, D. A.; Erickson, K.; Naujok, R.; Brostrom, M.; Mueller, M.; Chou, S.-H.; Young, V. G., Jr. *Inorg. Chem.* **2003**, *42*, 932.

(15) Hesse, N.; Fröhlich, R.; Humelnicu, I.; Würthwein, E.-U. *Eur. J. Inorg. Chem.* **2005**, 2189.

(16) Ley, H.; Müller, F. *Ber. Dtsch. Chem. Ges* **1907**, *40*, 2950.

(17) Breuer, S. W.; Small, R. W. H. *Acta Crystallogr.* **1991**, *C47*, 871.

(18) Walther, M.; Wermann, K.; Lutsche, M.; Günther, W.; Görls, H.; Anders, E. *J. Org. Chem.* **2006**, *71*, 1399.

(19) Baker, J.; Kilner, M.; Mahmoud, M. M.; Wallwork, S. C. *J. Chem. Soc., Dalton Trans.* **1989**, 837.

(20) Bokach, N. A.; Kuznetsova, T. V.; Simanova, S. A.; Haukka, M.; Pombeiro, A. J. L.; Kukushkin, V. Yu. *Inorg. Chem.* **2005**, *44*, 5152.

(21) Guo, J.-P.; Wong, W.-K.; Wong, W.-Y. *Eur. J. Inorg. Chem.* **2006**, 3634.

(22) Guo, J.-P.; Wong, W.-K.; Wong, W.-Y. *Eur. J. Inorg. Chem.* **2004**, 267.

(23) Turnbull, M. M.; Wei, M. Y.; Willett, R. D. *J. Coord. Chem.* **1995**, *35*, 11.

(24) Kajiwara, T.; Kamiyama, A. *Chem. Commun* **2002**, 1256. Kajiwara, T.; Kamiyama, A.; Ito, T. *Inorg. Chim. Acta* **2003**, *22*, 1789. Kamiyama, A.; Noguchi, T.; Kajiwara, T.; Ito, T. *Inorg. Chem.* **2002**, *41*, 507. Lerner, E. I.; Lippard, S. J. *J. Am. Chem. Soc.* **1976**, *98*, 5397.

(25) Kajiwara, T.; Ito, T. *Eur. J. Inorg. Chem.* **2004**, 3084.

(26) Kryatov, S. V.; Nazarenko, A. Y.; Smith, M. B.; Rybak-Akimova, E. V. *Chem. Commun.* **2001**, 1174.

(27) Guzei, I. A.; Crozier, K. R.; Nelson, K. J.; Pinkert, J. C.; Schoenfeldt, N. J.; Shepardson, K. E.; McGaff, R. W. *Inorg. Chim. Acta* **2006**, *359*, 1169.

(28) Norrestam, R. *Acta Crystallogr., Sect. C* **1984**, *40*, 955.

(29) Guedes da Silva, M. F. C.; Ferreira, C. M. P.; Branco, E. M. P. R. P.; Fraústo da Silva, J. J. R.; Pombeiro, A. J. L.; Michelin, R. A.; Belluco, U.; Bertani, R.; Mozzon, M.; Bombieri, G.; Benetollo, F.; Kukushkin, V. Yu. *Inorg. Chim. Acta* **1997**, *265*, 267 (Topical Volume on Platinum Chemistry)

(30) For reviews see: Kukushkin, V. Yu.; Pombeiro, A. J. L. *Chem. Rev.* **2002**, *102*, 1771. Pombeiro, A. J. L.; Kukushkin, V. Yu. Reactions of Coordinated Nitriles. In *Comprehensive Coordination Chemistry*, 2nd ed.; Elsevier: Amsterdam, 2004; Vol. 1, Chapter 1.34, pp 639–660.

(31) Gushchin, P. V.; Bokach, N. A.; Luzyanin, K. V.; Nazarov, A. A.; Haukka, M.; Kukushkin, V. Yu. *Inorg. Chem.* **2007**, *46*, 1684.

Scheme 1. Tailoring Reaction in the Temperature Range (A) from 20 to 40 °C (R = Me (**1**), Et (**2**), CH$_2$Ph (**3**), Ph (**4**)) and (B) from −20 to 4 °C (R = Et (**5**), CH$_2$Ph (**6**))

Scheme 2
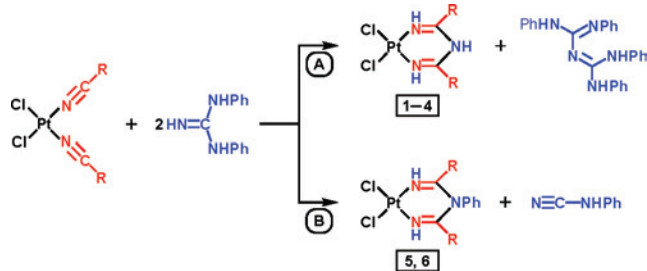
under mild conditions and afforded diimino compounds containing two N-bound monodentate 1,3-diaza-1,3-diene ligands, [PtCl$_2$\{NH=C(R)N=C(NMe$_2$)$_2$\}$_2$]; this reaction was the first observation of metal-mediated nucleophilic addition of a guanidine to ligated nitrile.

As a continuation of the project focused on the study of metal-mediated nitrile−guanidine interplay, we attempted the reaction between another guanidine, e.g. *N,N′*-diphenylguanidine (NH=C(NHPh)$_2$) and the Pt^{II} precursors and found that the process with NH=C(NHPh)$_2$ was strongly different from that with HN=C(NMe$_2$)$_2$. Indeed, at the cis-Pt^{II} centers a novel tailoring process is realized instead of the coupling, although at the trans-Pt^{II} centers the interaction follows the expected route; all of these processes will be considered below in separate sections.

Nitrile−Guanidine Coupling at the *cis*-(RCN)$_2$Pt^{II} Center. The tailoring reaction of the two adjacent nitrile ligands in *cis*-[PtCl$_2$(RCN)$_2$] (R = Me, Et, CH$_2$Ph, Ph) upon interaction with NH=C(NHPh)$_2$ in a 1:2 molar ratio proceeds in the corresponding RCN (for R = Me, Et) and in CH$_2$Cl$_2$ (for R = Ph, CH$_2$Ph) at 20–25 °C for 24 h or at 40 °C for 2 h and gives a 50–60% yield of Pt 1,3,5-triazapentadiene complexes **1–4** (Scheme 1, route A).

In all cases, the complexes were separated by filtration and the filtrates contain, as was verified by TLC, more than 10 as yet unidentified products. In addition to **1–4**, another major product formed in the reaction is, most likely, diphenylcarbodiimide PhN=C=NPh, but this heterocumulene is highly reactive and couples with HN=C(NHPh)$_2$ to give the biguanidine PhN=C(NHPh)N=C(NHPh)$_2$, which was detected by ESI$^+$-MS (*m/z* 406 [M + H]$^+$) (Scheme 1, route A); similar reactions between carbodiimides and various N-donor nucleophiles are well-known from the literature.[31,32] It is worth noticing that (i) we did not observe the higher molecular weight products, which may originate from further bis(guanidine) and (nitrile)Pt^{II} coupling, in accord with our previous findings[33] and (ii) N,N-chelating
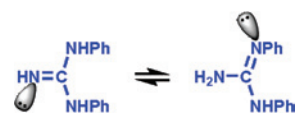
properties of the bis(guanidine) explain the insufficient selectivity of the tailoring: ESI$^+$-MS monitoring of the reaction mixture allows the detection of the bisguanidine chelation products (see the Experimental Section).

The reaction in CH$_2$Cl$_2$ proceeds differently at lower temperatures. When the reaction between *cis*-[PtCl$_2$(RCN)$_2$] (R = Et, CH$_2$Ph) and DPG in a 1:2 molar ratio starts at −20 °C followed by heating to 4 °C and keeping the mixture under this temperature for 1 day, the NH tailoring (compounds **2** and **3**; isolated yields are 35% and 26%, respectively) (Scheme 1, route A) is accompanied by the NPh tailoring, giving **5** and **6** in ca. 4% and 25% yields, respectively (Scheme 1, route B). Precipitates were weighed, fully dissolved in DMSO-*d$_6$*, and analyzed by ^{1}H NMR. The molar ratios **2:5** and **3:6** obtained by NMR integration are ca. 8:1 and ca. 1:1, respectively. Yields of **2** and **5** and of **3** and **6** were calculated on the basis of these ^{1}H NMR data. Another product of the route B (Scheme 1) is the known[34] phenylcyanamide (ESI$^-$-MS, *m/z* 117 [M − H]$^-$). In two other cases (i.e., R = Ph, Me), we were unable to isolate the NPh-tailoring products: first, the reaction of *cis*-[PtCl$_2$(PhCN)$_2$] with DPG at –20 °C in CH$_2$Cl$_2$ is not selective, and in addition, all products which were formed exhibit solubility too high to allow separation by fractional recrystallization; second, the very poor solubility of *cis*-[PtCl$_2$(MeCN)$_2$] prevented us from pursuing further studies.

It is worth noting that complex **6** could also be obtained at 20–25 °C in CH$_2$Cl$_2$ by the reaction of *cis*-[PtCl$_2$-(PhCH$_2$CN)$_2$] with DPG in a 1:4 molar ratio; however, the yield of solid product **6** (9%) is small and the filtrate contains a broad spectrum of as yet unidentified products. It was also found that **6** is not formed at all in the reaction between *cis*-[PtCl$_2$(PhCH$_2$CN)$_2$] and the guanidine in a 1:4 molar ratio at 20–25 °C in MeNO$_2$; in the latter case the only poorly soluble product is complex **3** (yield 33%). Consequently, one might assume that the selectivity of the tailoring reaction, i.e. NH vs NPh tailoring, of the two adjacent RCN nitrile ligands in *cis*-[PtCl$_2$(RCN)$_2$] depends on the solvent polarity. This viewpoint can be rationalized by the solvent-dependent tautomeric equilibrium of DPG[35] (Scheme 2; the left form predominates in polar solvents) and, consequently, by involvement of two different nucleophilic centers (NH vs NPh) in the initial step of the reaction.

A plausible mechanism (Scheme 3) of the tailoring involves nucleophilic attack of the Pt^{II}-activated nitrile by either the NH (route C) or NPh (route G) center and formation of the eight-membered chelates formed via routes

(32) Zhang, W.-X.; Nishiura, M.; Hou, Z. *Chem. Eur. J.* **2007**, *13*, 4037. Ma, L.; Zhang, J.; Cai, R.; Chen, Z.; Zhou, X. *Dalton Trans.* **2007**, *25*, 2718. Guiducci, A. E.; Boyd, C. L.; Mountford, P. *Organometallics* **2006**, *25*, 1167. Ding, M.-W.; Yang, S.-J.; Zhu, J. *Synthesis* **2004**, *1*, 75. Bell, S. A.; Meyer, T. Y.; Geib, S. J. *J. Am. Chem. Soc.* **2002**, *124*, 10698. Molina, P.; Alajarin, M.; Perez de Vega, M. J.; Lopez, A. *Heterocycles* **1989**, *29*, 1607. Ibrahim, I. T.; Williams, A. *J. Chem. Soc., Perkin Trans. 2* **1982**, *11*, 1455. Kurzer, F.; Douraghi-Zadeh, K. *J. Chem. Soc.* **1965**, 3912.

(33) Bokach, N. A.; Kukushkin, V. Yu.; Haukka, M.; Fraústo da Silva, J. J. R.; Pombeiro, A. J. L. *Inorg. Chem.* **2003**, *42*, 3602.

(34) Crutchley, R. J. *Compr. Coord. Chem. II* **2004**, *1*, 117. Crutchley, R. J. *Coord. Chem. Rev.* **2001**, *125*, 219–221.

(35) Bureiko, S. F.; Koll, A.; Przeslawska, M. *J. Struct. Chem.* **2002**, *43*, 412. Bocharov, V. N.; Bureiko, S. F.; Koll, A.; Rospenk, M. *J. Struct. Chem.* **1999**, *39*, 502. Koll, A.; Rospenk, M.; Bureiko, S. F.; Bocharov, V. N. *J. Phys. Org. Chem.* **1996**, *9*, 487. Clement, B.; Kaempchen, T. *Chem. Ber.* **1986**, *119*, 1101.

Scheme 3
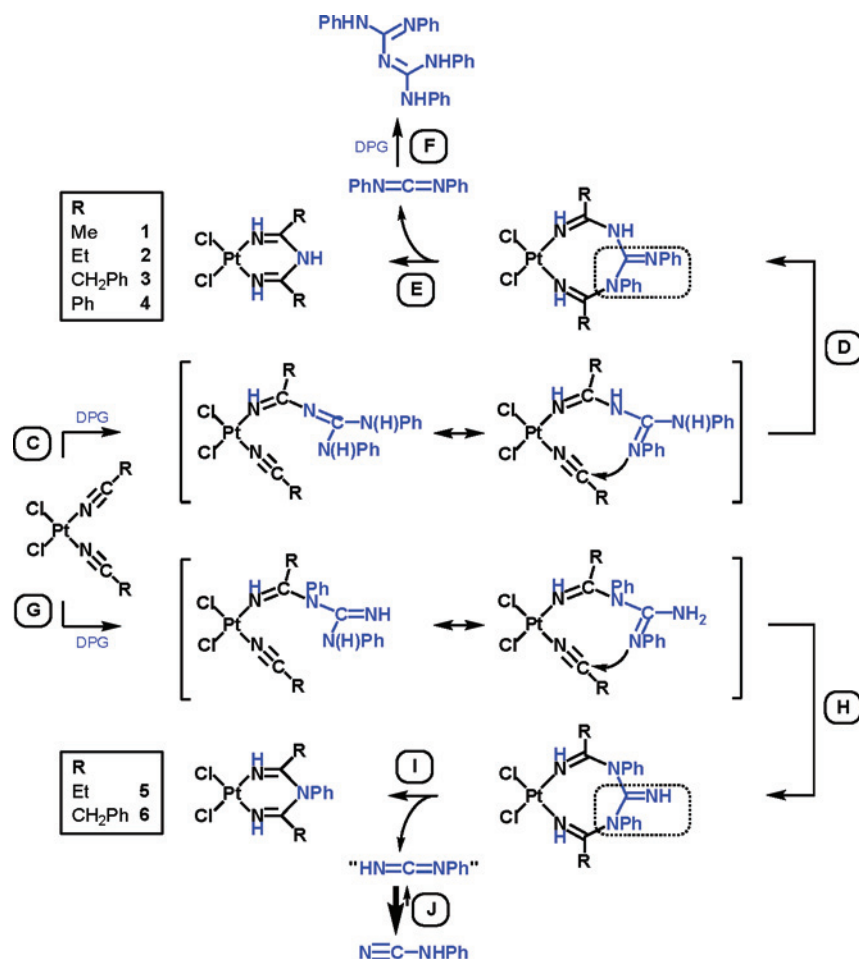
C/D and G/H. Although these chelates should be unstable, they could be isolated by us for the complexes *cis*-[PtCl₂-(RCN)₂] bearing highly conjugated RCN species, and these data will be published separately.[36] Extruding the carbodiimide and narrowing the chelate ring (routes E and I) gives the products of NH and NPh tailoring, respectively. The fate of the carbodiimide is different and depends on its nature. Thus, PhN=C=NPh couples with excess DPG (route F), yielding the bis(guanidine), while HN=C=NPh rapidly tautomerizes[37] to the nitrile NCN(H)Ph (route J), which is unreactive toward DPG.

Thus, we can see that the guanidine NH=C(NHPh)₂ reacts with *cis*-(RCN)₂Pt^II centers and serves as the NH₂R¹-tailoring reagent (R¹ = H, Ph) for the two adjacent nitrile ligands in *cis*-[PtCl₂(RCN)₂] (R = Me, Et, CH₂Ph, Ph) at 20–25 °C (R¹ = H) or at −20 °C (R¹ = Ph).

Different Reactivity Modes of the *cis*-(EtCN)₂Pt^II Moiety and DPG or NH₃. Being interested in the amplification of the tailoring reaction to other (RCN)₂Pt^II complexes, we decided to apply the reaction with DPG for the *N,N,N′,N′*-

tetramethylethylenediamine (tmeda) complex *cis*-[Pt(tmeda)-(EtCN)₂][SO₃CF₃]₂ (**8**·(OTf)₂; prepared from **7**[38] via route K, Scheme 4). It is important that the tmeda chelation provides exclusive cis arrangement of the nitrile species, thus making the complex **8**·(OTf)₂ a convenient model for studying the tailoring reaction with DPG as well as for comparison of reactivity modes between the *cis*-(EtCN)₂Pt^II moiety and DPG vs NH₃.

When a dichloromethane solution of **8**·(OTf)₂ was treated with an excess of gaseous ammonia at 20−25 °C for 6 h (Scheme 4, route L), the formation of the platinum(II) bis(amidine) complex *cis*-[Pt(tmeda){NH=C(NH₂)Et}₂]-[SO₃CF₃]₂ (**9**·(OTf)₂) was observed and it was isolated in 85% yield; the ammination proceeds in accord with previous observations.[39–45] ¹H NMR monitoring proved the absence of the tailoring product [Pt(tmeda){NH=C(Et)}₂NH]-[SO₃CF₃]₂ (**10**·(OTf)₂) in the reaction mixture. In contrast,

(36) Gushchin, P. V.; Bokach, N. A.; Haukka, M.; Kukushkin, V. Yu. Unpublished work.

(37) Boyer, J. H.; Frints, P. J. A. *J. Heterocycl. Chem.* **1970**, *7*, 71; *Chem. Abstr.* **1970**, *72*, 90378. Lempert, K.; Puskas, J.; Bekassy, S. *Period. Polytech., Chem. Eng.* **1968**, *12*, 123; *Chem. Abstr.* **1969**, *70*, 11239.

(38) Monti, E.; Gariboldi, M.; Maiocchi, A.; Marengo, E.; Cassino, C.; Gabano, E.; Osella, D. *J. Med. Chem.* **2005**, *48*, 857.

(39) Kukushkin, V. Yu.; Aleksandrova, E. A.; Kukushkin, Yu. N. *Zh. Obshch. Khim.* **1995**, *65*, 1937; *Chem. Abstr.* **1996**, *125*, 24936.

(40) Kukushkin, Yu. N.; Aleksandrova, E. A.; Pakhomova, T. B. *Zh. Obshch. Khim.* **1994**, *64*, 151; *Chem. Abstr.* **1994**, *122*, 121719.

(41) Kukushkin, Yu. N.; Aleksandrova, E. A.; Pakhomova, T. B.; Vlasova, R. A. *Zh. Obshch. Khim.* **1994**, *64*, 705; *Chem. Abstr.* **1995**, *121*, 147636.

(42) Longato, B.; Bandoli, G.; Mucci, A.; Schenetti, L. *Eur. J. Inorg. Chem.* **2001**, 3021.
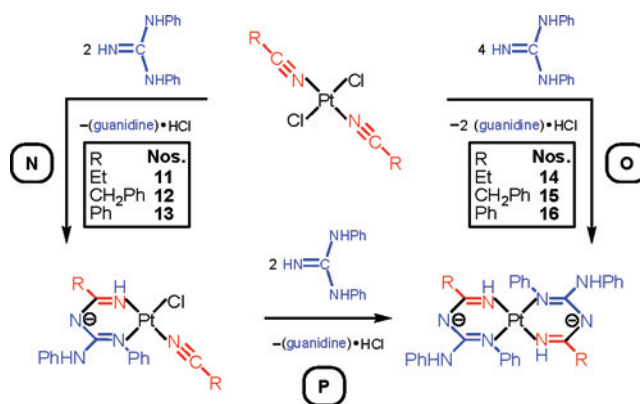
Scheme 4
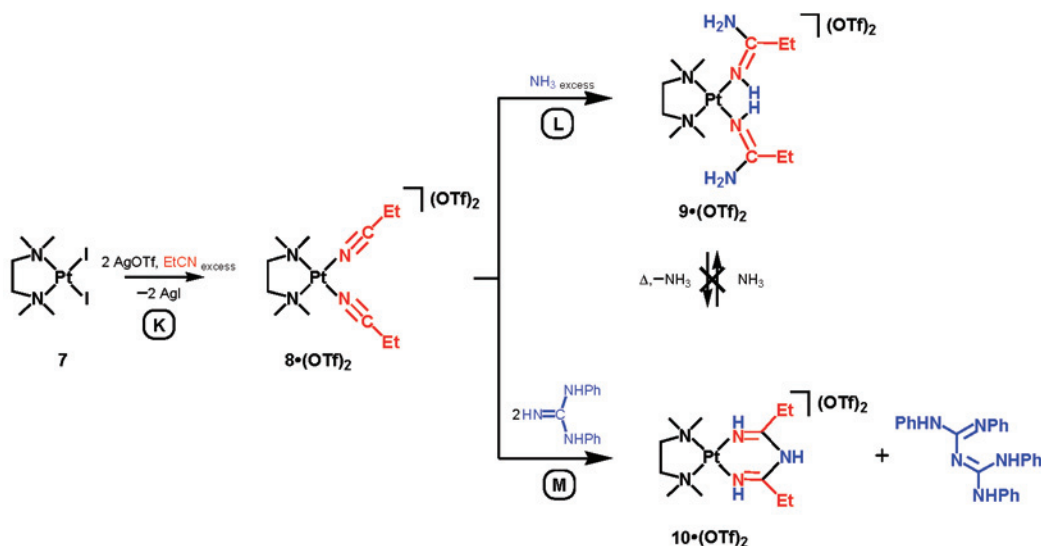
Scheme 5

the reaction of **8**·(OTf)$_2$ and DPG performed under similar conditions (Scheme 4, route M) led to the (1,3,5-triazapentadiene)Pt^{II} complex **10**·(OTf)$_2$, derived from the tailoring reaction, and no **9**·(OTf)$_2$ was detected in the reaction mixture.

Moreover, in separate experiments it was established that (i) the chelate **10**·(OTf)$_2$ did not react with ammonia in a methanolic solution (6 h, 20–25 °C) to give **9**·(OTf)$_2$ and (ii) the bis(amidine) complex **9**·(OTf)$_2$ did not convert to **10**·(OTf)$_2$ upon heating either in solution (24 h, 100 °C, MeNO$_2$) or in the solid state (gradual decomposition from ca. 115 °C on TG; see Figure S1 in the Supporting Information). These observations (Scheme 4, routes L and M) indicate the unique character of the reaction and point out that the role of DPG is more complicated and does not come from the donation of ammonia in the novel tailoring reaction, thus additionally supporting the plausible mechanism depicted in Scheme 3.

Nitrile−Guanidine Coupling at the *trans*-(RCN)$_2$Pt^{II} Center. The complex *trans*-[PtCl$_2$(MeCN)$_2$] exhibits poor solubility in most noncoordinating solvents, and the reaction between DPG and the more soluble *trans*-[PtCl$_2$(RCN)$_2$] (R = Et, CH$_2$Ph, Ph) was studied. Treatment of *trans*-[PtCl$_2$(RCN)$_2$] (R = Et, CH$_2$Ph, Ph) with 2 equiv of DPG in EtCN (R = Et) or CH$_2$Cl$_2$ (R = CH$_2$Ph, Ph) solutions at 20–25 °C for 15–24 h resulted in formation of [PtCl{*N*H=C(R)NC(NHPh)=*N*Ph}(RCN)] (**11–13**), which were isolated in 45, 26, and 20% yields, respectively, by taking the reaction mixture to dryness, followed by washing of the solid residue with MeOH (R = Et) or after column chromatography on SiO$_2$ (R = CH$_2$Ph, Ph); in all three cases solutions also

contain a broad mixture of as yet unidentified compounds. Complexes **11–13** formed as products of the nucleophilic addition of DPG to the nitrile carbon atom, followed by ring closure of the formed 1,3,5-triazapentadiene ligand (Scheme 5, route N). It is noteworthy that when *trans*-[PtCl$_2$(RCN)$_2$] (R = Et, CH$_2$Ph, Ph) reacts with 2 equiv of DPG at room temperature, complexes **14–16** (see below) are not formed.

A further increase in the amount of DPG from 2 to 3 equiv decreases the yield of **11–13** to ca. 10%. The yield of **11** is higher if the solvent is the corresponding nitrile rather than CH$_2$Cl$_2$ or CHCl$_3$ (45% when the reaction is carried out in EtCN vs 20% in CH$_2$Cl$_2$). Unfortunately, the preparation of **12** and **13** in PhCH$_2$CN or PhCN, respectively, is not practical due to the low volatility of these solvents and difficulties in crystallizing the final products.

When *trans*-[PtCl$_2$(RCN)$_2$] (R = Et, CH$_2$Ph, Ph) react in the corresponding nitrile RCN with 4 equiv of DPG for a prolonged reaction time (1–2 days) at 75 °C (Scheme 5, route O) or **11–13** are treated with 2 equiv more of DPG at the same temperature (Scheme 5, route P), complexes containing two bidentate 1,3,5-triazapentadiene ligands, i.e. [Pt{*N*H=C(R)NC(NHPh)=*N*Ph}$_2$] (**14–16**), are formed and they are isolated in 63–73% yields. Thus, the reaction of DPG and the *trans*-(RCN)$_2$Pt complexes follows the expected path

(43) Belluco, U.; Benetollo, F.; Bertani, R.; Bombieri, G.; Michelin, R. A.; Mozzon, M.; Tonon, O.; Pombeiro, A. J. L.; Guedes da Silva, F. C. *Inorg. Chim. Acta* **2002**, *334*, 437.

(44) Belluco, U.; Benetollo, F.; Bertani, R.; Bombieri, G.; Michelin, R. A.; Mozzon, M.; Pombeiro, A. J. L.; Guedes da Silva, F. C. *Inorg. Chim. Acta* **2002**, *330*, 225.

(45) Natile, G.; Intini, F. P.; Bertani, R.; Michelin, R. A.; Mozzon, M.; Sbovata, S. M.; Venzo, A.; Seraglia, R. *J. Organomet. Chem.* **2005**, *690*, 2121.
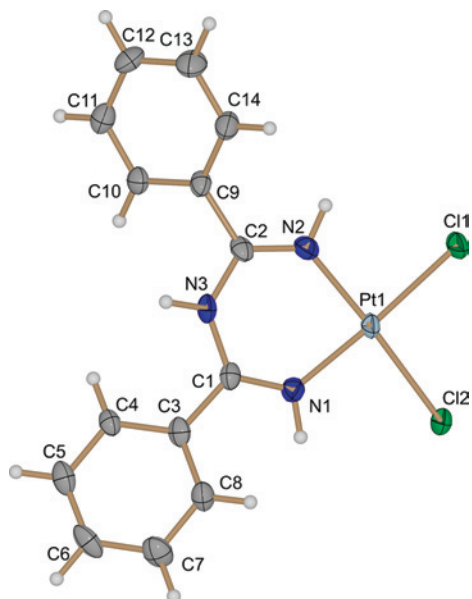
Figure 1. Thermal ellipsoid view of complex **4** with the atomic numbering scheme. Thermal ellipsoids are drawn at the 50% probability level.

previously established by us for the metal-mediated nitrile–amidine coupling.[20]

Characterization of (1,3,5-triazapentadiene)Pt^{II} Complexes. The formulation of complexes **1–4**, **9·(OTf)₂**, **10·(OTf)₂**, and **11–16** was supported by satisfactory C, H, and N elemental analyses, in agreement with FAB⁺ (**1–3**, **9·(OTf)₂**, **11–16**), ESI⁺-MS (**5**, **6**, **8·(OTf)₂**, **10·(OTf)₂**), and ESI⁻-MS (**1–6**) data. In the IR spectra, (1,3,5-triazapentadiene/ato)Pt^{II} (**1–4**), **10·(OTf)₂**, **11–16**, and also the (amidine)₂Pt^{II} complex **9·(OTf)₂** display strong ν(C=N) or ν(C=N and/or C=C) bands in the range 1672–1442 cm⁻¹. The structures of **1**, **2**, **4**, **11**, **13**, and **14** and picrates of complexes **9²⁺** and **10²⁺** were determined by single-crystal X-ray diffraction.

(A) Complexes 1–4. Comparison of the IR spectra of **1–4** with those of the starting materials indicates the absence of the C≡N stretching vibrations and the presence of strong ν(C=N) bands in the range 1672–1539 cm⁻¹ and N–H stretching vibrations, which emerge at higher frequencies (3396–3043 cm⁻¹). A characteristic feature of the ¹H NMR spectra of **1–4** is the availability of two singlets with 1:2 intensities from the NH protons at 11.28–10.65 and 10.22–9.45 ppm, respectively. The position of the signals at such a low field gives indirect evidence that the NH proton is involved in hydrogen bonding in solution.[46] The most downfield signal in the region of 11.28–10.65 ppm corresponds to the proton at the central N atom.

The structures of **1**, **2**, and **4** were determined by X-ray single-crystal diffraction (Figure 1 and Figures S2 and S3 in the Supporting Information), and it was observed that they

all have square-planar geometry. In **1**, **2**, and **4**, atoms forming the metallacycles lie in one plane with the rms deviations 0.009(3) (**1**), 0.059(3) (**2**), and 0.064(5) Å (**4**). The CN bonds in the metallacycles of **1**, **2**, and **4** have a low degree of delocalization. The bond lengths N(1)–C(1), N(2)–C(2) in **1**, **2**, and **4** are 1.287(4), 1.285(4) Å, 1.287(5), 1.281(5) Å, and 1.289(7), 1.286(7), 1.297(7), 1.298(7), 1.281(7), 1.291(7) Å, respectively (Table 1). These values are closer to the C=N double-bond value and comparable with the corresponding C=N double bonds of the bis-cationic (1,3,5-triazapentadiene/ato)Ni^{II} complex [Ni{NH=C(R)NHC-(R)=NH}₂]²⁺ (1.282(3)–1.294(3) Å).[10] The bond lengths N(3)–C(1), N(3)–C(2) in **1**, **2**, and **4** are 1.363(4), 1.374(4) Å, 1.368(4), 1.379(4) Å, and 1.391(7), 1.366(7), 1.378(7), 1.374(7), 1.386(7), 1.376(8) Å, respectively. These values are closer to the C–N single-bond value and comparable with the corresponding C–N single-bond values of the bis-cationic (1,3,5-triazapentadiene/ato)Ni^{II} complex [Ni{NH=C(R)NHC(R)=NH}₂]²⁺ (1.357(4)–1.374(4) Å).[10] In **4**, the adjacent molecules are linked by weak (NH···Cl) interactions (Figure S5 and Table S1 in the Supporting Information).

(B) Complexes 9·(OTf)₂ and 10·(OTf)₂. In the IR spectra of **9·(OTf)₂** and **10·(OTf)₂**, the Pt^{II}-bound amidine and 1,3,5-triazapentadiene ligands exhibit medium-to-strong bands at 3439–3242 cm⁻¹, which can be attributed to the N–H stretching vibrations, and display no bands in the region specific to ν(C≡N) stretches. The IR spectrum of **9·(OTf)₂** shows C=N absorption bands in the range between 1659 and 1616 cm⁻¹ characteristic of amidine ligands, while for **10·(OTf)₂**, the ν(C=N) peaks of the 1,3,5-triazapentadiene ligand appear as two strong bands at 1610 and 1547 cm⁻¹. The latter values are lower than those for the (amidine)₂Pt^{II} complex **9·(OTf)₂**, and this fact can be rationalized by a conjugation (although of low degree; see later discussion on the X-ray structures) within the 1,3,5-triazapentadienyl chelating system.

The amidine resonances of **9·(OTf)₂** are observed in the ¹H NMR spectrum as broad singlets in a 1:1:1 ratio at 6.68 ppm for the imino (HN=C) protons and at 7.07 and 7.43 ppm for the amido (H₂NC) protons; we believe these sets of signals are related to the existence of a few conformational forms in solution. In the ¹H NMR spectrum of **10·(OTf)₂**, NH resonances moved to low field and emerged at 10.94 ppm for the proton at the central N atom and at 9.22 ppm for the imino protons (HN=C) in a 1:2 ratio. In the ¹³C{¹H} NMR spectra, the carbons from the N=C–N moiety were detected at ca. 174 ppm for **9·(OTf)₂** and at ca. 164 ppm for **10·(OTf)₂**.

Complexes **9²⁺** and **10²⁺** were isolated as the picrates, and these two salts give crystals suitable for X-ray diffraction studies (Figure 2, Table 2). The Pt–N$_{tmeda}$ bonds in **9²⁺** (2.059(6), 2.074(5) Å) and **10²⁺** (2.071(3), 2.078(3) Å) and the Pt–N$_{imine}$ bonds in **9²⁺** (1.997(5), 1.999(5) Å) and **10²⁺** (1.987(3), 1.991(3) Å) agree well with each other and with those found in [Pt{NH=C(NH₂)NMe₂}(dien)][SO₃CF₃]₂ (dien = diethylenetriamine) (2.036(6)–2.049(6) Å for

(46) Makarycheva-Mikhailova, A. V.; Haukka, M.; Bokach, N. A.; Garnovskii, D. A.; Galanski, M.; Keppler, B. K.; Pombeiro, A. J. L.; Kukushkin, V. Yu. *New J. Chem.* **2002**, *26*, 1085. Kukushkin, V. Yu.; Pakhomova, T. B.; Bokach, N. A.; Wagner, G.; Kuznetsov, M. L.; Galanski, M.; Pombeiro, A. J. L. *Inorg. Chem.* **2000**, *39*, 216. Kukushkin, V. Yu.; Pakhomova, T. B.; Kukushkin, Yu. N.; Herrmann, R.; Wagner, G.; Pombeiro, A. J. L. *Inorg. Chem.* **1998**, *37*, 6511.
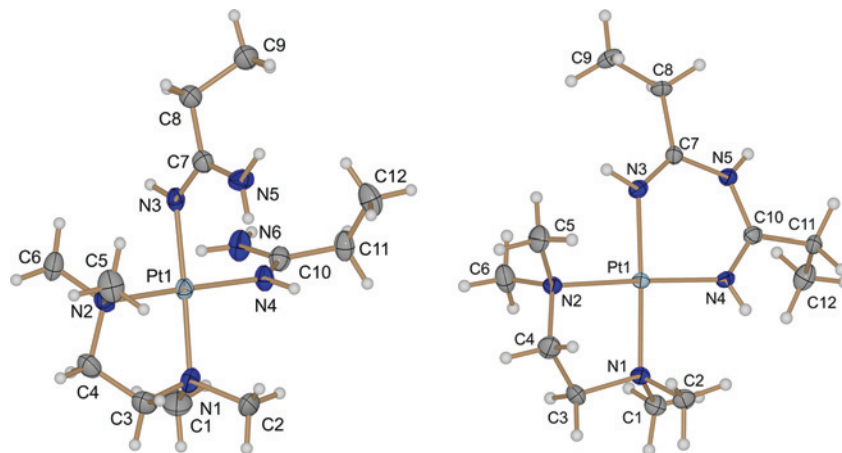
Figure 2. Thermal ellipsoid views of complexes $\mathbf{9^{2+}}$ (left) and $\mathbf{10^{2+}}$ (right) with the atomic numbering scheme. Thermal ellipsoids are drawn at the 50% probability level. The picrate anions are omitted for simplicity.

Table 1. Selected Bond Lengths (Å) and Angles (deg) for **1**, **2**, and **4**

	1	**2**	**4A**[a]	**4B**[a]	**4C**[a]
Pt(1)−N(1)	1.965(2)	1.969(3)	1.965(5)	1.975(4)	1.959(5)
Pt(2)−N(2)	1.964(3)	1.971(3)	1.960(5)	1.970(5)	1.968(5)
Pt(1)−Cl(1)	2.3250(8)	2.3139(8)	2.3167(14)	2.3174(13)	2.3144(15)
Pt(1)−Cl(2)	2.3190(8)	2.3226(8)	2.3121(14)	2.3146(14)	2.3071(14)
N(1)−C(1)	1.287(4)	1.287(5)	1.289(7)	1.297(7)	1.281(7)
N(2)−C(2)	1.285(4)	1.281(5)	1.286(7)	1.298(7)	1.291(7)
N(3)−C(1)	1.363(4)	1.368(4)	1.391(7)	1.378(7)	1.386(7)
N(3)−C(2)	1.374(4)	1.379(4)	1.366(7)	1.374(7)	1.376(8)
N(1)−Pt(1)−N(2)	89.66(10)	89.63(12)	89.4(2)	89.4(2)	89.5(2)
Cl(1)−Pt(1)−Cl(2)	93.93(3)	92.65(3)	95.72(5)	92.56(5)	94.51(5)
C(1)−N(3)−C(2)	129.1(3)	128.7(3)	127.8(5)	127.9(5)	128.0(5)

[a] The asymmetric unit of **4** contains three independent molecules.

**Table 2.** Selected Bond Lengths (Å) and Angles (deg) for $\mathbf{9^{2+}}$ and $\mathbf{10^{2+}}$

	$\mathbf{9^{2+}}$	$\mathbf{10^{2+}}$
Pt(1)−N(1)	2.059(6)	2.071(3)
Pt(1)−N(2)	2.074(5)	2.078(3)
Pt(1)−N(3)	1.999(5)	1.991(3)
Pt(1)−N(4)	1.997(5)	1.987(3)
N(1)−C(3)	1.494(9)	1.505(5)
N(2)−C(4)	1.494(8)	1.495(5)
N(3)−C(7)	1.299(8)	1.282(5)
N(5)−C(7)	1.326(8)	1.364(5)
C(3)−C(4)	1.491(10)	1.493(6)
N(1)−Pt(1)−N(2)	85.6(2)	85.31(12)
N(3)−Pt(1)−N(4)	88.3(2)	88.08(12)
N(3)−C(7)−N(5)	120.9(6)	122.0(3)

Pt−N$_{dien}$ and 1.997(6), 2.018(7) Å for Pt−N$_{imine}$).[47] The C=N bond lengths in (amidine)$_2$Pt^{II}(tmeda) (1.288(8) and 1.299(8) Å) and (1,3,5-triazapentadiene)Pt^{II}(tmeda) (1.279(5) and 1.282(5) Å) and the C−N bond lengths (1.326(8) and 1.340(8) Å and 1.364(5) and 1.371(5) Å, respectively) have values typical for the (amidine)$_2$Pt^{II} complexes[43,44] and for the (1,3,5-triazapentadiene)Pt^{II} complexes, listed above, and correspond, within 3σ, with each other. Therefore, the bond lengths are statistically equivalent within the two classes of ligands, and differences between complexes $\mathbf{9^{2+}}$ and $\mathbf{10^{2+}}$ are observed only in their spectra.

(47) Fairlie, D. P.; Jackson, W. G.; Skelton, B. W.; Wen, H.; White, A. H.; Wickramasinghe, W. A.; Woon, T. C.; Taube, H. *Inorg. Chem.* **1997**, *36*, 1020.

(C) Complexes 11−16. The IR spectra of these compounds display strong ν(C=N and/or C=C) bands at 1636–1442 cm^{-1} and N−H stretching vibrations in the range of 3422−3338 cm^{-1}. These ranges agree well with values of ν(C=N and/or C=C) (1632−1430 cm^{-1}) and ν(N−H) (3395–3282 cm^{-1}) bands for the (1,3,5-triazapentadiene/ato)Pt^{II} complexes [PtCl(NCR){*N*H=C(R)NC(Ph)*N*(Ph)}] and [Pt{*N*H=C(R)NC(Ph)*N*(Ph)}$_2$] (Et, CH$_2$Ph, Ph).[20] The weak C≡N stretching vibrations are present in the IR spectra for compounds **11−13** but not in those for complexes **14−16**. This can be rationalized by the fact that **14−16** are products of the nucleophilic addition of DPG to both nitriles RCN of *trans*-[PtCl$_2$(RCN)$_2$] (R = Et, CH$_2$Ph, Ph), while **11−13** are formed in the reaction incorporating one ligand RCN of *trans*-[PtCl$_2$(RCN)$_2$] (R = Et, CH$_2$Ph, Ph) with DPG. The characteristic feature of ^{1}H NMR spectra of the (1,3,5-triazapentadiene/ato)Pt^{II} complexes **11−16** is the presence of two singlets due to the NH protons in the range of 6.50–4.84 ppm.

The structures of **11**, **13**, and **14** were determined by single-crystal X-ray diffraction (Figures 3 and 4, Table 3, and Figure S4 in the Supporting Information). They all have square-planar geometry. In **11**, the disordered coordinated nitrile is bent (N(4)−C(3)−C(4A) = 168.4(6)° and N(4)−C(4)−C(4B) = 154.9(6)°), probably because of the steric repulsion from the aromatic ring of the chelated ligand, while in **13** the nitrile fragment is linear (N(4)−C(3)−C(4) = 179.0(7)°). The bond lengths of N(3)−C(2) in **11** and
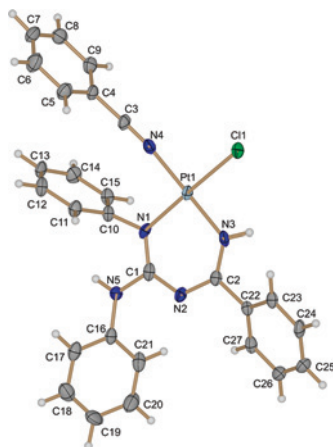
Figure 3. Thermal ellipsoid view of complex **13** with the atomic numbering scheme. Thermal ellipsoids are drawn at the 50% probability level.
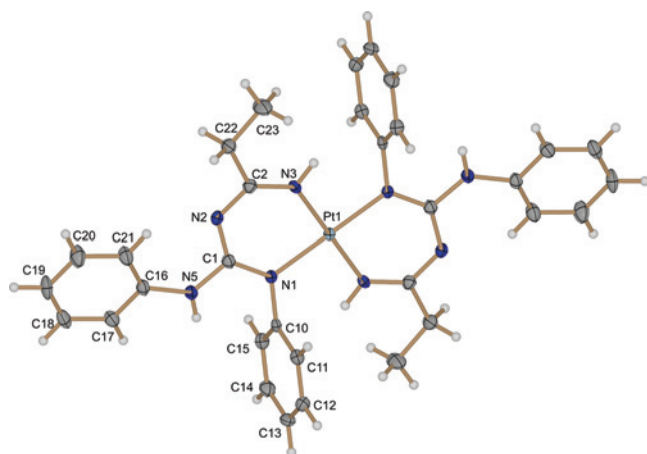

Figure 4. Thermal ellipsoid view of complex **14** with the atomic numbering scheme. Thermal ellipsoids are drawn at the 50% probability level.

Table 3. Selected Bond Lengths (Å) and Angles (deg) for **11**, **13**, and **14**

	11	**13**	**14**
Pt(1)−N(1)	2.017(2)	2.001(5)	2.039(2)
Pt(1)−N(3)	1.952(3)	1.941(5)	1.990(2)
Pt(1)−N(4)	2.001(3)	1.979(5)	
Pt(1)−Cl(1)	2.3112(8)	2.3169(15)	
N(1)−C(1)	1.330(4)	1.354(8)	1.339(3)
N(2)−C(1)	1.346(4)	1.345(8)	1.332(3)
N(2)−C(2)	1.333(4)	1.352(8)	1.344(3)
N(3)−C(2)	1.313(4)	1.330(8)	1.306(3)
N(5)−C(1)	1.370(4)	1.372(8)	1.381(3)
N(5)−C(16)	1.414(4)	1.422(8)	1.414(3)
N(4)−C(3)	1.115(5)	1.154(8)	
C(3)−C(4)		1.434(8)	
C(3)−C(4A)[a]	1.489(7)		
C(3)−C(4B)[a]	1.605(12)		
N(1)−Pt(1)−N(3)	88.76(10)	89.6(2)	87.23(8)
Cl(1)−Pt(1)−N(4)	89.14(8)	90.26(15)	
C(1)−Pt(1)−C(2)	123.3(3)	121.9(5)	122.8(2)
C(1)−N(5)−C(16)	128.9(2)	127.9(5)	130.5(2)
Pt(1)−N(4)−C(3)	174.8(3)	172.9(5)	

[a] In **11**, C(4) is disordered over two sites.

N(3)−C(2) in **14** (1.313(4) and 1.306(3) Å, respectively) have values typical for the corresponding N=C bonds in both Pt[II] and Ni[II] 1,3,5-triazapentadiene/ato complexes[10,20] and, within 3σ, the N=C bond in compounds with the
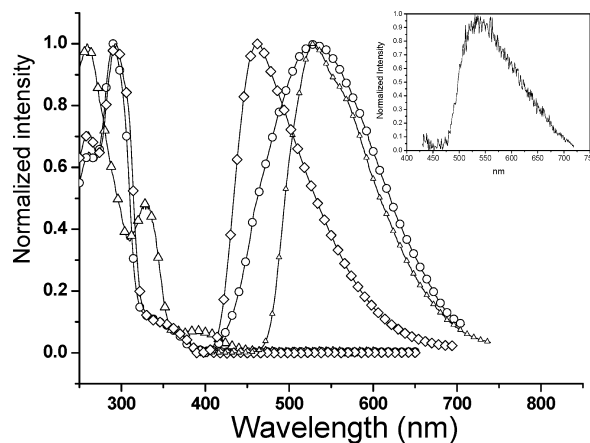
Figure 5. Absorption spectra in CH₂Cl₂ and the normalized solid-state emission spectra of **14** (○), **15** (□), and **16** (△). Inset: emission spectrum of **16** in CH₂Cl₂. The excitation wavelength is set at 350 nm. All measurements were performed at 25 °C.

$C_{Ar}-C=N-C$ moiety[48] (mean value 1.279(8) Å). The bond lengths N(2)−C(2) and N(2)−C(1) in **11** (1.333(4) and 1.346(4) Å, respectively) and in **14** (1.344(3) and 1.332(3) Å, respectively) have values closer to the corresponding N−C bonds in both (1,3,5-triazapentadiene/ato)M (M = Pt[II], Ni[II]) complexes.[10,20] The bond lengths N(1)−C(1) in **11** (1.330(4) Å) and in **14** (1.339(3) Å) are longer than the corresponding N=C bond lengths in both (1,3,5-triazapentadiene/ato)M (M = Pt[II], Ni[II]) complexes,[10,20] which can be related to the influence of the NHPh group. However, all values still remain typical, within 3σ, for such types of 1,3,5-triazapentadiene/ato metallacycles. The N=C and N−C bond lengths in the metallacycles **11** and **14**, in contrast to the case for (1,3,5-triazapentadiene/ato)M (M = Pt[II], Ni[II]),[10,20] exhibit a greater degree of delocalization in the ring. The distinct distribution of double and single CN bonds in the metallacycle **13** is vague (the bond lengths N(3)−C(2), N(2)−C(2), N(2)−C(1), and N(1)−C(1) are 1.330(8), 1.352(8), 1.345(8), and 1.354(8) Å, respectively); it has a greater degree of the delocalization in comparison to **11** and **14** and a significantly higher degree of delocalization as compared with Pt[II] and Ni[II] 1,3,5-triazapentadiene/ato complexes.[10,20] In **11**, **13**, and **14** the atoms of the metallacycles lie in one plane with rms deviations 0.094(3) (**11**), 0.061(5) (**13**), and 0.143(2) Å (**14**).

Photophysical Data for 14–16 and Theoretical Approaches for Their Interpretation. Focus of this section is mainly on complexes **14–16**, due to their unique structures and great luminescence intensity in the solid state (vide infra). The absorption and luminescence spectra have been recorded for **14–16** in CH₂Cl₂ and in the solid state. The associated spectra are depicted in Figure 5, and pertinent data are summarized in Table 4. In general, the high-energy absorption bands at <300 nm for **14–16** can be reasonably assigned to the 1,3,5-triazapentadiene ππ* transition. The next lower energy band with a shoulder at ~350 nm (390 nm for **16**) is assigned to the spin-allowed metal-to-ligand charge transfer (¹MLCT) transition, due to its relatively lower absorptivity. Supplementary support of these assignments is also provided

(48) Allen, F. H.; Kennard, O.; Watson, D. G.; Brammer, L.; Orpen, A. G.; Taylor, R. *J. Chem. Soc., Perkin Trans. 2* **1987**, S1.

Table 4. Photophysical Properties of **14–16**

	λ_{abs} (nm)[a]	$\lambda_{emission}$, nm[b]	Φ_f[b]	τ_{obs} (μs)[b]	τ_r (μs)[b]
14	295, 353	530	0.39	2.62	6.72[b]
15	290, 351	460	0.61	3.69	6.04[b]
16	315, 380	530	0.74	0.82	1.10[b]
		535	0.007[c]	0.01[c]	1.71[c]

[a] The absorption spectrum was acquired in CH_2Cl_2. [b] Measurements were perfomed in the solid state. τ_{obs} and τ_r denote the observed and radiative decay times, respectively. [c] Data were recorded in degassed CH_2Cl_2 solution using three freeze–pump–thaw cycles.

by the computational approaches (vide infra). We unfortunately could not resolve any emission for complexes **14** and **15** in degassed CH_2Cl_2 solutions at room temperature, while a weak emission (quantum yield $\Phi_f \approx 7 \times 10^{-3}$) was resolved with a peak wavelength at ~535 nm (see inset of Figure 5). Taking into account the sensitivity of the current detection system, the emission yield for **14** and **15**, if there is any, is concluded to be less than 10^{-5}. Such an observation is similar to the case for many Pt^{II} complexes, which are emissive in the solid state, whereas they are nonemissive in fluid solutions at room temperature.[49] The title Pt complexes are in a square-planar configuration and possess an empty d orbital perpendicular to the plane. The empty orbital is subject to coordination by electron donors in the solvent, resulting in a dominant radiationless transition. The quenching processes associated with e.g. solvent collision and/or large amplitude motions can be drastically reduced in the form of a solid film. Supporting evidence is provided by the strong emission acquired in the solid state for the studied complexes, with Φ_f being measured to be 0.39, 0.61, and 0.74 for **14**−**16**, respectively (see Figure 5 and Table 4). Knowing that $\Phi_f \times \tau_r = \tau_{obs}$, where τ_{obs} and τ_r denote the measured and radiative lifetimes, respectively, τ_r for **14**–**16** can thus be calculated and are given in Table 4. Clearly, the deduced radiative lifetime of microseconds for all **14**–**16** confirms the origin of emission from the triplet manifold: i.e., phosphorescence.[50,51] Furthermore, the short radiative lifetime, in combination with the lack of vibronic progression in emission spectra, manifests the T_1−S_0 transition to be MLCT mixed, in part, with $\pi\pi^*$ character. For complex **16**, the emission spectrum in view of peak wavelength and spectral features in CH_2Cl_2 is similar to that in the solid film. Since **16** should exist in a well-dispersed, monomeric form in CH_2Cl_2, it is thus reasonable to conclude negligible intermolecular Pt−Pt nonbonding interactions for **16** in the solid film. Knowing such interactions frequently take place in Pt^{II} complexes,[52] the negligible Pt^{II} packing interaction in solid films can possibly be rationalized by the overall nonplanar structure, avoiding significant intermolecular interaction.
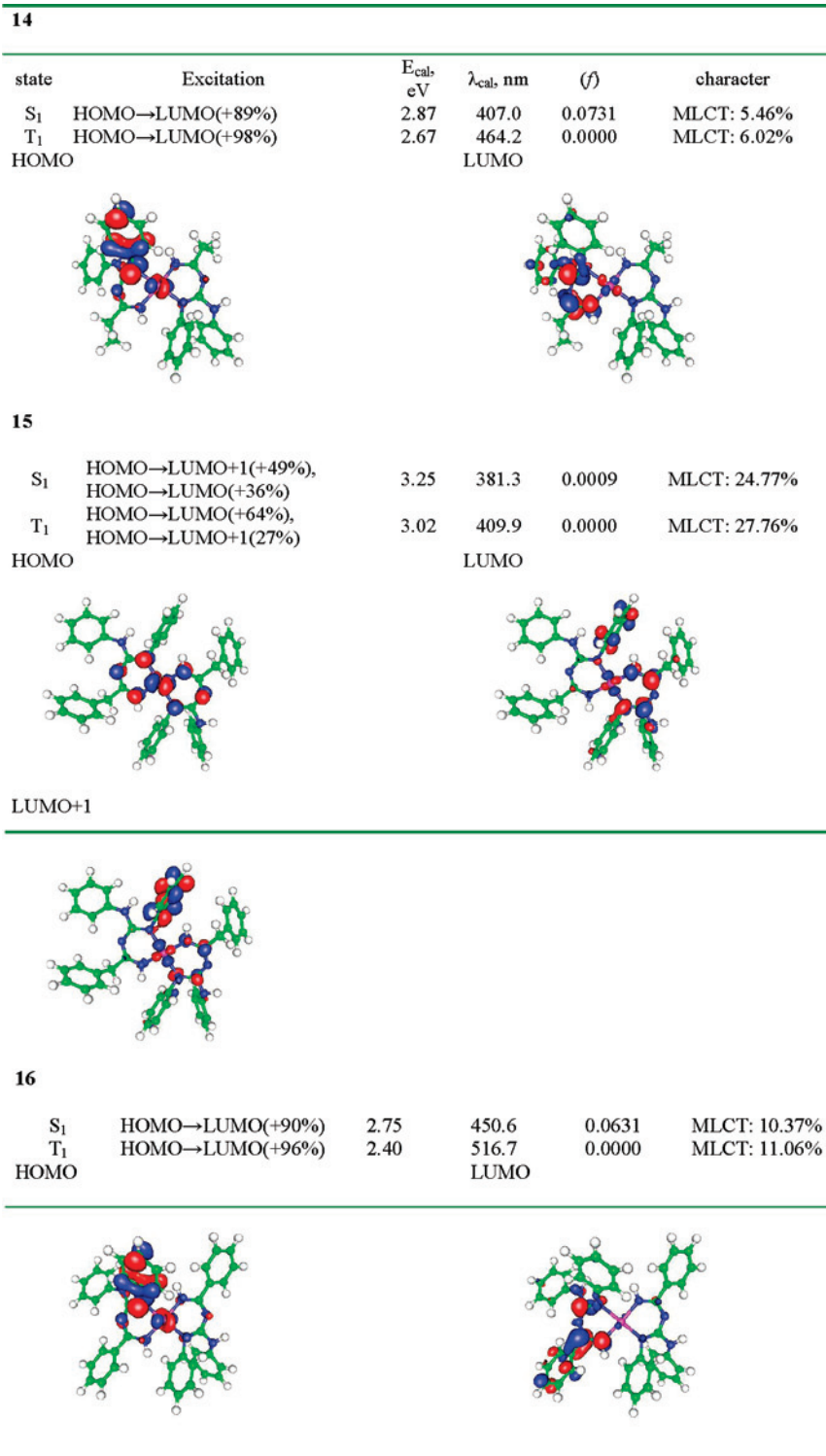
(49) Kui, S. C. F.; Chui, S. S. Y.; Che, C. M.; Zhu, N. *J. Am. Chem. Soc.* **2006**, *128*, 8297.

(50) Chang, S.-Y.; Kavitha, J.; Hung, J.-Y.; Chi, Y.; Cheng, Y.-M.; Li, E. Y.; Chou, P.-T.; Lee, G.-H.; Carty, A. J. *Inorg. Chem.* **2007**, *46*, 7064.

(51) Scaffidi-Domianello, Y. Yu.; Nazarov, A. A.; Haukka, M.; Galanski, M.; Keppler, B. K.; Schneider, J.; Du, P.; Eisenberg, R.; Kukushkin, V. Yu. *Inorg. Chem.* **2007**, *46*, 4469.

(52) Chang, S.-Y.; Kavitha, J.; Li, S.-W.; Hsu, C.-S.; Chi, Y.; Yeh, Y.-S.; Chou, P.-T.; Lee, G.-H.; Carty, A. J.; Tao, Y.-T.; Chien, C.-H. *Inorg. Chem.* **2006**, *45*, 137.

To gain more insight into the above photophysical behavior, the electronic transition properties calculations of **14**–**16** were performed using density functional theory method (DFT). With the use of the TD-B3LYP method incorporating the obtained geometries from the structural optimization calculations, the vertical (i.e., Franck–Condon) excitation energy from the ground state to the lowest lying electronic excited state in both singlet and triplet manifolds was calculated. The TDDFT results are summarized in Figure 6. Clearly, the calculated S_1 and T_1 energy levels for the title complexes are qualitatively consistent with the 0–0 onset of the absorption (S_1) and phosphorescence (T_1) spectra. Thus, the theoretical level adopted here should be suitable for studying the photophysical properties of these complexes in a qualitative manner. As shown in Figure 6, the transitions to S_1 and T_1 are mainly attributed to the HOMO → LUMO transition for complexes **14** and **16,** while the excitation, in part, also involves the HOMO → LUMO+1 transition for complex **15**. The frontier orbitals, HOMO, and LUMO for **14**–**16** are also depicted in Figure 6. Evidently, the HOMO → LUMO transition for all the complexes involves metal to ligand charge transfer (MLCT) and part of the ligand $\pi\pi^*$ character. For complexes **14** and **15**, the transitions also incorporate certain degrees of the dd* transition. Knowing that a dd* transition normally causes weakness of the metal–ligand bonding strength, the results may partially account for the nonemissive properties of complexes **14** and **15** in CH_2Cl_2. Further support is given by complex **16**. In sharp contrast to complexes **14** and **15**, the lowest lying state of complex **16** involves negligible dd* transition and hence **16** exhibits a relatively higher quantum yield of 0.007 in CH_2Cl_2. It is also noteworthy that a similar dd* transition may not cause drastic radiationless quenching in the solid state due to the confinement of the lattice energy.

Final Remarks

The results from this work can be summarized into three perspectives. First, the tailoring reaction between two cis-ligated RCN species represents a novel reactivity mode, which has never been reported at any metal center. Although this synthetic transformation was demonstrated only for nitriles at Pt^{II} centers, we anticipate amplifying this type of reaction to RCN ligands at other metal centers and extending the application to, for example various homoleptic nitrile hard or soft metal complexes.[53] Second, the tailoring reaction constitutes a facile route to the trinitrogen analogues of the 1,3-dicarbonyls, i.e., Pt 1,3,5-triazapentadienyl complexes. Despite increasing interest in the latter systems, relevant reports are rare, mainly because the synthetic methods so far are rather poorly developed. Third, bis(1,3,5-triazapentadiene)Pt^{II} complexes such as **14**–**16** are found to exhibit strong luminescence in the solid state, raising the future possibility that these systems may be useful for sensing or

(53) Davies, J. A.; Hockensmith, C. M.; Kukushkin, V. Yu.; Kukushkin, Yu. N. *Synthetic Coordination Chemistry: Principles and Practice*; World Scientific: Singapore, 1996; pp 95–156.

14

state	Excitation	E_{cal}, eV	λ_{cal}, nm	(f)	character
S$_1$	HOMO→LUMO(+89%)	2.87	407.0	0.0731	MLCT: 5.46%
T$_1$	HOMO→LUMO(+98%)	2.67	464.2	0.0000	MLCT: 6.02%
HOMO			LUMO		

15

state	Excitation	E_{cal}, eV	λ_{cal}, nm	(f)	character
S$_1$	HOMO→LUMO+1(+49%), HOMO→LUMO(+36%)	3.25	381.3	0.0009	MLCT: 24.77%
T$_1$	HOMO→LUMO(+64%), HOMO→LUMO+1(27%)	3.02	409.9	0.0000	MLCT: 27.76%
HOMO			LUMO		

LUMO+1

16

state	Excitation	E_{cal}, eV	λ_{cal}, nm	(f)	character
S$_1$	HOMO→LUMO(+90%)	2.75	450.6	0.0631	MLCT: 10.37%
T$_1$	HOMO→LUMO(+96%)	2.40	516.7	0.0000	MLCT: 11.06%
HOMO			LUMO		

Figure 6. Descriptions, energy gaps, oscillation strengths of S$_1$ and T$_1$, and HOMO and LUMO of **14–16**.

display applications, upon proper derivatization. Work focusing on these projects is underway in our group.

Experimental Section

Materials and Instrumentation. The guanidine HN=C(NHPh)$_2$ (Aldrich) and solvents were obtained from commercial sources and used as received. The complexes *cis*-[PtCl$_2$(RCN)$_2$] (R = Me,[54] Et[55]) were prepared in accord with the published methods. These compounds contain admixtures of the trans isomers (an isomeric cis:trans ratio obtained by NMR integration is ca. 5:1 for R = Me[54] and ca. 6:1 for R = Et[55]). The isomerically pure complexes *trans*-[PtCl$_2$(RCN)$_2$] (R = Et,[55] CH$_2$Ph[56]) and *cis*-[PtCl$_2$(PhCH$_2$CN)$_2$][56] were obtained as previously described. The complex *trans*-[PtCl$_2$(PhCN)$_2$] was obtained upon heating

(54) Fanizzi, F. P.; Intini, F. P.; Maresca, L.; Natile, G. *J. Chem. Soc., Dalton Trans.* **1990**, 199.
(55) Svensson, P.; Lövqvist, K.; Kukushkin, V. Yu.; Oskarsson, Å. *Acta Chem. Scand.* **1995**, *49*, 72. Kukushkin, V. Yu.; Oskarsson, Å.; Elding, L. I. *Inorg. Synth.* **1997**, *31*, 279.

Table 5. Crystal Data

	1	2	4	9^{2+}	10^{2+}	11	13	14
empirical formula	$C_4H_9Cl_2N_3Pt$	$C_6H_{13}Cl_2N_3Pt$	$C_{90}H_{92}Cl_{12}N_{18}O_3Pt_6$	$C_{24}H_{36}N_{12}O_{14}Pt$	$C_{24}H_{33}N_{11}O_{14}Pt$	$C_{19}H_{22}ClN_5Pt$	$C_{27}H_{22}ClN_5Pt$	$C_{32}H_{34}N_8Pt$
fw	365.13	393.18	3069.76	911.74	894.70	550.96	647.04	725.76
temp (K)	120(2)	120(2)	120(2)	120(2)	120(2)	150(2)	120(2)	120(2)
λ (Å)	0.710 73	0.710 73	0.710 73	0.710 73	0.710 73	0.710 73	0.710 73	0.710 73
cryst syst	monoclinic	monoclinic	monoclinic	triclinic	monoclinic	triclinic	triclinic	Ttriclinic
space group	$P2_1/c$	$P2_1/n$	$P2_1/c$	$P\bar{1}$	$P2/c$	$P\bar{1}$	$P\bar{1}$	$P\bar{1}$
a (Å)	16.0700(12)	7.0744(2)	18.8625(11)	8.8755(4)	23.7788(6)	10.2632(3)	9.1616(5)	5.9465(2)
b (Å)	9.8856(8)	10.9430(2)	16.8259(3)	12.8837(4)	8.25930(10)	10.4416(3)	10.1225(4)	11.2920(3)
c (Å)	12.9953(8)	13.4809(3)	16.1677(4)	15.8393(9)	16.7947(5)	10.9637(3)	13.6355(8)	12.0993(4)
α (deg)	90	90	90	79.692(3)	90	64.084(2)	99.329(3)	109.305(1)
β (deg)	123.432(3)	101.901(1)	103.071(1)	84.415(2)	104.5010(10)	85.286(2)	105.703(2)	101.928(2)
γ (deg)	90	90	90	71.220(3)	90	67.6680(10)	93.557(3)	103.712(2)
V (Å³)	1722.9(2)	1021.19(4)	4998.3(3)	1685.58(13)	3193.34(13)	972.52(5)	1193.75(11)	707.99(4)
Z	8	4	2	2	4	2	2	1
ρ_{calcd} (Mg/m³)	2.815	2.557	2.040	1.796	1.861	1.881	1.800	1.702
μ (Mo Kα) (mm³)	16.840	14.215	8.742	4.246	4.480	7.364	6.015	4.992
no. of rflns	10 483	19 450	90 669	25 566	36 698	17 081	18 018	9087
no. of unique rflns	1972	2338	11 421	6362	7314	4428	5210	3225
R_{int}	0.0293	0.0488	0.0557	0.0568	0.0562	0.0324	0.0656	0.0362
R1^a ($I \geq 2\sigma$)	0.0156	0.0185	0.0335	0.0384	0.0319	0.0195	0.0419	0.0178
wR2^b ($I \geq 2\sigma$)	0.0281	0.0432	0.0644	0.0946	0.0586	0.0486	0.0932	0.0426

^{a} R1 $= \sum ||F_o| - |F_c||/\sum |F_o|$. ^{b} wR2 $= [\sum[w(F_o^2 - F_c^2)^2]/\sum[w(F_o^2)^2]]^{1/2}$.

[PtCl$_2$(MeCN)$_2$] with PhCN,[57] followed by separation of the admixture of the cis isomer by column chromatography on SiO$_2$ (silica gel 60 F$_{254}$, 0.063–0.200 mm, Merck; eluent is 1/20 (v/v) ethyl acetate−CHCl$_3$, R_f for the trans isomer is 0.68). The *cis*-[PtCl$_2$(PhCN)$_2$] complex was separated from the cis/trans isomeric mixture, which was obtained in the reaction[58] between K$_2$[PtCl$_4$] and PhCN in water, by column chromatography on SiO$_2$ (silica gel 60 F$_{254}$, 0.063–0.200 mm, Merck; eluent 1/20 ethyl acetate−CHCl$_3$, R_f for the cis isomer is 0.31). TLC was done on Merck 60 F$_{254}$ SiO$_2$ plates.

Elemental analyses were obtained on a Hewlett-Packard 185B carbon hydrogen nitrogen analyzer. DTA/TG measurements were performed using a Perkin-Elmer (Diamond TG/DTA) derivatograph in air at a heating rate of 10 °C/min (carrier gas air, 200 mL/min). ESI-TOF mass spectra were obtained on a MX-5310 mass spectrometer. Positive-ion FAB mass spectra of the platinum(II) complexes were obtained on a MS-50C (Kratos) instrument by bombarding 3-nitrobenzyl alcohol matrices of the samples with 8 keV (ca. 1.28×10^{15} J) Xe atoms. Mass calibration for data system acquisition was achieved using CsI. Infrared spectra (4000–400 cm^{-1}) were recorded on a Shimadzu FTIR 8400S instrument in KBr pellets. ^{1}H and ^{13}C{^{1}H} NMR spectra were measured on a Bruker-DPX 300 spectrometer at ambient temperature.

X-ray Crystal Structure Determinations. The crystals were immersed in cryo oil and mounted in a nylon loop, and the data were measured at a temperature of 120 or 150 K. The X-ray diffraction data were collected by means of a Nonius KappaCCD diffractometer using Mo Kα radiation ($\lambda = 0.710 73$ Å). The Denzo-Scalepack[59] and EvalCCD[60] program packages were used for cell refinements and data reductions. All of the structures were solved by direct methods using *SHELXS-97*,[61] *SIR2002*, or *SIR2004* with the WinGX[62] graphical user interface. An empirical absorption correction was applied to all of the data (*SADABS*[63] or *XPREP* in *SHELXTL*[64]). Structural refinements were carried out using *SHELXL-97*.[65] The asymmetric unit of **4** contains three independent Pt molecules, an acetone molecule, and half of a water molecule. In **11** the carbon atoms C(4) and C(5) were disordered over two sites with occupancies 0.43/0.57. In **1**, **2**, **4**, **9^{2+}**, **10^{2+}**, **11**, and **14** the NH and H$_2$O hydrogen atoms were located from the difference Fourier map but constrained to ride on their parent atom with U_{iso} being 1.5 times the U_{eq} value for the parent atom. Other hydrogens were positioned geometrically and constrained to ride on their parent atoms, with C−H = 0.95–0.99 Å, N−H = 0.88 Å, and U_{iso} being 1.2–1.5 times the U_{eq} value for the parent atom. The crystallographic details are summarized in Table 5, and selected bond lengths and angles in Tables 1−3.

Luminescence Study of 14–16. Steady-state absorption and emission spectra were recorded by a Hitachi (U-3310) spectrophotometer and an Edinburgh (FS920) fluorimeter, respectively. Both the wavelength-dependent excitation and emission responses of the fluorimeter were calibrated. A configuration of the front-face excitation was used to measure the emission of the solid sample, for which the cell was made by assembling two edge-polished quartz plates with various Teflon spacers. A combination of appropriate filters was used to avoid interference from the scattering light. An integrating sphere (Labsphere) was applied to measure the quantum yield in the solid state, with excitation by a 365 nm Ar$^+$ laser line. The resulting luminescence was acquired with a charge-coupled device (Princeton Instruments, Model CCD-1100) for subsequent quantum yield analyses. Lifetime studies were performed with an Edinburgh FL 900 photon-counting system with a hydrogen-filled or nitrogen lamp as the excitation source.

Theoretical Methodology. All calculations were done with the Gaussian 03 program.[66] The geometries of complexes **14–16** were

(56) Kukushkin, V. Yu.; Tkachuk, V. M.; Vorobiov-Desiatovsky, N. V. *Inorg. Synth.* **1998**, *32*, 144.
(57) Makarycheva-Mikhailova, A. V.; Bokach, N. A.; Kukushkin, V. Yu.; Kelly, P. F.; Gilby, L. M.; Kuznetsov, M. L.; Holmes, K. E.; Haukka, M.; Parr, J.; Stonehouse, J. M.; Elsegood, M. R. J.; Pombeiro, A. J. L. *Inorg. Chem.* **2003**, *42*, 301.
(58) Fanizzi, F. P.; Intini, F. P.; Natile, G. *J. Chem. Soc., Dalton Trans.* **1989**, 947.
(59) Otwinowski, Z.; Minor, W. Processing of X-ray Diffraction Data Collected in Oscillation Mode. In *Methods in Enzymology*; Carter, C. W., Sweet, J., Eds.; Academic Press: New York, 1997; Vol. 276, Macromolecular Crystallography, Part A, pp 307–326.
(60) Duisenberg, A. J. M.; Kroon-Batenburg, L. M. J.; Schreurs, A. M. M. *J. Appl. Crystallogr.* **2003**, *36*, 220–229.
(61) Sheldrick, G. M. *SHELXS-97, Program for Crystal Structure Determination*, University of Göttingen, Göttingen, Germany, 1997.
(62) Farrugia, L. J. *J. Appl. Crystallogr.* **1999**, *32*, 837.
(63) Sheldrick, G. M. *SADABS - Bruker Nonius Scaling and Absorption Correction, v 2.10*; Bruker AXS, Inc., Madison, WI, 2003.
(64) Sheldrick, G. M. *SHELXTL v. 6.14-1*; Bruker AXS, Inc., Madison, WI, 2005.
(65) Sheldrick, G. M. *SHELXL-97, Program for Crystal Structure Refinement*; University of Göttingen, Göttingen, Germany, 1997.

calculated by the hybrid DFT B3LYP functional.[67] Except for the platinum element, the split-valence basis set 6-31G* was chosen to describe the other elements. The pseudopotential LANL2 combines a valence double-ζ basis set; i.e., LANL2DZ was chosen for platinum in order to describe its relativistic effect.[68] All minima were identified positively, as the number of imaginary frequencies is zero. On the basis of the converged geometries, the vertical excitation energies were calculated by TDB3LYP with the same basis set mentioned above.[69]

Synthetic Work. Reaction of *cis*-[PtCl₂(RCN)₂] and DPG (2 equiv). HN=C(NHPh)₂ (53 mg, 0.25 mmol) was added to a solution of *cis*-[PtCl₂(RCN)₂] (0.12 mmol) in MeCN (1.2 mL; R = Me), EtCN (1 mL; R = Et), or CH₂Cl₂ (1 mL; R = CH₂Ph, Ph), and the mixture was left to stand for 2 h at 40 °C and then (for digestion of the initially formed precipitate) for 22 h at 20–25 °C (R = Me, Et) (crystals started to release already after 5−10 min) or 24 h at 20–25 °C (R = CH₂Ph, Ph) (pale yellow precipitate immediately began to release for R = CH₂Ph). Pale yellow crystals (R = Me, Et) or a pale yellow precipitate (R = CH₂Ph) was filtered off, washed with two 0.5 mL portions of Me₂CO and one 0.5 mL portion of Et₂O, and dried in air at 20–25 °C. The greenish yellow solution formed for R = Ph was evaporated to dryness, and the green oily residue was crystallized under a layer of hexane (1 mL) to form the solid yellow powder, which was washed with two 1 mL portions of Et₂O, dissolved in CHCl₃, purified by column chromatography on SiO₂ (silica gel 60 F₂₅₄, 0.063–0.200 mm, Merck; eluent 1/10 Me₂CO−CHCl₃, R_f = 0.40), and dried in air at 20–25 °C. Yields are 19 mg, 44% (R = Me), 25 mg, 54% (R = Et), 36 mg, 58% (R = CH₂Ph), and 17 mg, 30% (R = Ph).

1. Anal. Calcd for C₄H₉N₃Cl₂Pt: C, 13.16; H, 2.48; N, 11.51. Found: C, 13.19; H, 2.48; N, 11.59. ESI⁻-MS (*m/z*): 364 [M − H]⁻. FAB⁺-MS (*m/z*): 388 [M + Na]⁺, 365 [M]⁺, 329 [M − Cl]⁺. TLC: R_f = 0.69 (eluent 1/5 MeOH−CHCl₃). IR (KBr, selected bands, cm⁻¹): 3338 (m), 3282 (s), 3248 (s), 3149 (s), 3043 (m-s), ν(N−H); 2989 (m), ν(N−H and/or C−H from Me); 2773 (m-w), ν(C−H from Me); 1672 (s), 1545 (s), ν(C=N). ¹H NMR (DMSO-d_6, δ): 10.86 (s, 1H, N*H*), 9.94 (s, br, 2H, N*H*=CMe), 1.90 (s, 6H, C*H₃*). ¹³C{¹H} NMR (DMSO-d_6, δ): 152.37 (*C*=N), 21.59 (*C*H₃). Crystals suitable for an X-ray diffraction study were obtained directly from the reaction mixture.

2. Anal. Calcd for C₆H₁₃N₃Cl₂Pt: C, 18.32; H, 3.31; N, 10.68. Found: C, 18.76; H, 3.38; N, 10.65. ESI⁻-MS (*m/z*): 392 [M − H]⁻. FAB⁺-MS (*m/z*): 416 [M + Na]⁺, 393 [M]⁺, 357 [M − Cl]⁺, 321 [M − HCl - Cl]⁺. TLC: R_f = 0.43 (eluent 1/10 MeOH−CHCl₃). IR (KBr, selected bands, cm⁻¹): 3325 (m), 3284 (s), 3234 (s), 3140

(s), ν(N−H); 3028 (m), ν(N−H and/or C−H from Et); 2993 (m), 2978 (m), 2941 (m), 2879 (m-w), 2758 (m-w), ν(C−H from Et); 1664 (s), 1543 (s), ν(C=N). ¹H NMR (DMSO-d_6, δ): 10.87 (s, 1H, N*H*), 9.87 (s, br, 2H, N*H*=CEt), 2.39 (q, 7.3 Hz, 4H, C*H₂*), 1.09 (t, 7.3 Hz, 6H, C*H₃*) (*Et*). ¹³C{¹H} NMR (DMSO-d_6, δ): 157.26 (*C*=N), 28.73 (*C*H₂), 11.73 (*C*H₃) (*Et*). Crystals suitable for an X-ray diffraction study were obtained directly from the reaction mixture.

3. Anal. Calcd for C₁₆H₁₇N₃Cl₂Pt: C, 37.15; H, 3.31; N, 8.12. Found: C, 37.02; H, 3.39; N, 7.91. ESI⁻-MS (*m/z*): 516 [M − H]⁻. FAB⁺-MS (*m/z*): 556 [M + K]⁺, 540 [M + Na]⁺, 517 [M]⁺, 482 [M − Cl]⁺. TLC: R_f = 0.33 (eluent 1/10 MeOH−CHCl₃). IR (KBr, selected bands, cm⁻¹): 3309 (m-s), 3256 (m-s), 3166 (m-s), ν(N−H); 3043 (m), ν(N−H and/or C−H from Ar); 2908 (m-w), 2732 (w), ν(C−H from C*H₂*Ph); 1672 (s), ν(C=N); 1592 (w), 1543 (m-s), ν(C=N and/or C=C from Ar); 745 (m-s), 701 (s), δ(C−H from Ar). ¹H NMR (DMSO-d_6, δ): 11.28 (s, 1H, N*H*), 10.22 (s, 2H, N*H*=CCH₂Ph), 7.31 (s, 10H, Ph), 3.78 (s, 4H, C*H₂*Ph). ¹³C{¹H} NMR (DMSO-d_6, δ): 154.13 (*C*=N), 134.28 (*C*ipso), 129.53, 129.36, 126.13 (carbons in Ph).

4·2½H₂O. The hydrate was obtained using undried solvents, and the isolated solid was dried in air at 20–25 °C. Anal. Calcd for C₁₄H₁₃N₃Cl₂Pt·2½H₂O: C, 31.52; H, 3.40; N, 7.88. Found: C, 31.78; H, 3.65; N, 8.07. ESI⁻-MS (*m/z*): 488 [M − H]⁻. TLC: R_f = 0.40 (eluent 1/5 Me₂CO−CHCl₃). IR (KBr, selected bands, cm⁻¹): 3396 (w), 3347 (w), 3233 (m-w), ν(N−H); 3057 (m-w), ν(N−H and/or C−H from Ph); 1624 (s), ν(C=N); 1594 (s), 1539 (s), ν(C=N and/or C=C from Ar); 755 (m-s), 695 (s), δ(C−H from Ar). ¹H NMR (Me₂CO-d_6, δ): 10.65 (s, br, 1H, N*H*), 9.45 (s, br, 2H, N*H*=CPh), 7.94 (d, 4H, *o*-Ph), 7.72 (t, 2H, *p*-Ph), 7.57 (t, 4H, *m*-Ph). ¹³C{¹H} NMR (CDCl₃, δ): 157.67 (*C*=N), 136.68 (*C*ipso), 129.61, 129.04, 126.77 (carbons in Ph). Crystals of [PtCl₂-{*N*HC(Ph)NHC(Ph)=*N*H}]₃·Me₂CO·½H₂O suitable for an X-ray diffraction study were obtained by slow evaporation at 20–25 °C of a CH₂Cl₂−Me₂CO (1/1, v/v) solution.

Reaction of *cis*-[PtCl₂(RCN)₂] (R = Et, CH₂Ph, Ph) and DPG (2 equiv) at −20 °C. *cis*-[PtCl₂(RCN)₂] (R = Et, CH₂Ph, Ph) (0.12 mmol) and HN=C(NHPh)₂ (52.7 mg, 0.25 mmol) were dissolved in CH₂Cl₂ at −20 °C and left to stand for 2 h with slow heating to 4 °C, and then the reaction mixture was kept for 24 h at 4 °C. The pale yellow precipitate that formed was filtered off, washed with two 0.5 mL portions of CH₂Cl₂, and one 0.5 mL portion of Et₂O, and dried in air at 20–25 °C. It was weighed, fully dissolved in DMSO-d_6, and analyzed by ¹H NMR. Molar ratios of complexes **2** and **5** and of **3** and **6** obtained by the NMR integration are ca. 8:1 and ca. 1:1, respectively. Yields of **2**, **5**, **3**, and **6** were calculated on the basis of ¹H NMR data. The yields are 35% (**2**) and 4% (**5**), 26% (**3**), and 26% (**6**). In the case of *cis*-[PtCl₂-(PhCN)₂], the conductance of the reaction with DPG at −20 °C in CH₂Cl₂ led to formation of the tailoring product formulas. The latter exhibit very high solubility, and they were not isolated as solids but were characterized in the solution by ESI-MS.

5. We did not obtain sufficient amount of this material (see Results and Discussion) to conduct C, H, N analyses. ESI⁺-MS (*m/z*): 492 [M + Na]⁺, 508 [M + K]⁺. ESI⁻-MS (*m/z*): 392 [M − Ph]⁻. ¹H NMR (DMSO-d_6, δ): 10.28 (s, br, 2H, N*H*), 7.58 (m, 2H), 7.67 (m, 3H) (Ph), 2.03 (q, 7.5 Hz, 4H, C*H₂*), 0.83 (t, 7.5 Hz, 6H, C*H₃*) (*Et*).

6. We did not obtain sufficient amount of this material (see Results and Discussion) to conduct C, H, N analyses. ESI⁺-MS (*m/z*): 616 [M + Na]⁺. ESI⁻-MS (*m/z*): 516 [M − Ph]⁻. ¹H NMR (DMSO-d_6, δ): 10.55 (s, br, 2H, N*H*), 7.36 (t, 1H), 7.15 (t, 2H), 6.93 (d, 2H) (Ph), 7.22 (t, 6H), 6.73 (d, 4H) (CH₂*Ph*), 3.46 (s, 4H,

(66) Frisch, M. J.; Trucks, G. W.; Schlegel, H. B.; Scuseria, G. E.; Robb, M. A.; Cheeseman, J. R.; Montgomery, J. A. Jr.; Vreven, T.; Kudin, K. N.; Burant, J. C.; Millam, J. M.; Iyengar, S. S.; Tomasi, J.; Barone, V.; Mennucci, B.; Cossi, M.; Scalmani, G.; Rega, N.; Petersson, G. A.; Ehara, M.; Toyota, K.; Hada, M.; Fukuda, R.; Hasegawa, J.; Ishida, M.; Nakajima, T.; Kitao, O.; Nakai, H.; Honda, Y.; Nakatsuji, H.; Li, X.; Knox, J. E.; Hratchian, H. P.; Cross, J. B.; Adamo, C.; Jaramillo, J.; Cammi, R.; Pomelli, C.; Gomperts, R.; Stratmann, R. E.; Ochterski, J.; Ayala, P. Y.; Morokuma, K.; Salvador, P.; Dannenberg, J. J.; Zakrzewski, V. G.; Dapprich, S.; Daniels, A. D.; Strain, M. C.; Farkas, O.; Malick, D. K.; Rabuck, A. D.; Raghavachari, K.; Foresman, J. B.; Ortiz, J. V.; Cui, Q.; Baboul, A. G.; Clifford, S.; Cioslowski, J.; Stefanov, B. B.; Liu, G.; Liashenko, A.; Piskorz, P.; Komaromi, I.; Martin, R. L.; Fox, D. J.; Keith, T.; Al-Laham, M. A.; Peng, C. Y.; Nanayakkara, A.; Challacombe, M.; Gill, P. M. W.; Johnson, B.; Chen, W.; Wong, M. W.; Gonzalez, C.; Pople, J. A. *Gaussian 03, version A.1*; Gaussian, Inc., Pittsburgh, PA, 2002.
(67) (a) Becke, A. D. *Phys. Rev. A* **1988**, *38*, 3098. (b) Lee, C.; Yang, W.; Parr, R. G. *Phys. Rev. B* **1988**, *37*, 785.
(68) Hay, P. J.; Wadt, W. R. *J. Chem. Phys.* **1985**, *82*, 299.
(69) Stratmann, R. E.; Scuseria, G. E.; Frisch, M. J. *J. Chem. Phys.* **1998**, *109*, 8218.

CH_2Ph). ^{13}C{^{1}H} NMR (DMSO-d_6, δ): 156.01 (C=N), 137.80, 130.77 (C_{ipso}), 133.18, 131.14, 129.62, 129.40, 128.90, 128.12 (carbons in Ar), 42.97 (CH$_2$Ph).

Reaction of *cis*-[PtCl$_2$(RCN)$_2$] (R = Et, CH$_2$Ph, Ph) and DPG (4 equiv) at 20–25 °C. *cis*-[PtCl$_2$(PhCH$_2$CN)$_2$] (0.12 mmol) and HN=C(NHPh)$_2$ (52.7 mg, 0.25 mmol) were dissolved in CH$_2$Cl$_2$ and left to stand for 24 h at 20–25 °C. The pale yellow precipitate that formed was filtered off, washed with two 0.5 mL portions of Me$_2$CO and one 0.5 mL portion of Et$_2$O, and dried in air at 20–25 °C. The yield of **6** is 6 mg, 9%. The filtrate, as verified by means of both ^{1}H NMR and TLC methods, contains a broad mixture of as yet unidentified products but does not contain **6**. It was determined by ESI-MS that the filtrates contain products of the NH tailoring with substitution of two chloride Cl$^-$ ligands by the bis(guanidine) PhN=C(NHPh)N=C(NHPh)$_2$ (*m/z* 743 [M + H$_2$O]$^+$, 727 [M + 2H]$^+$, 708 [M − NH$_3$]$^+$, 672 [M + 2H − EtCN]$^+$ (R = Et); 868 [M + H$_2$O]$^+$, 850 [M]$^+$ (R = CH$_2$Ph); 839 [M + H$_2$O]$^+$, 822 [M + H]$^+$ (R = Ph)) and substitution of one Cl$^-$ ligand by HN=C(NHPh)$_2$ (*m/z* 569 [M + H]$^+$ (R = Et); 693 [M + H]$^+$, 691 [M − H]$^-$ (R = CH$_2$Ph); 665 [M + H]$^+$; 663 [M − H]$^-$ (R = Ph)).

Synthesis of [Pt(tmeda)(EtCN)$_2$]$^{2+}$ and Its Reaction with NH$_3$ and DPG. 7. This compound was obtained by the reaction of K$_2$[PtCl$_4$] with KI followed by the addition of tmeda (yield 86%; see the Supporting Information).[38] TLC on Merck 60 F$_{254}$ SiO$_2$ plates: R_f = 0.39 (eluent CHCl$_3$−Me$_2$CO, 5/2 v/v), one spot. IR (KBr, selected bands, cm^{-1}): 3016 (m-w), 2974 (m-w), 2914 (s) ν(N−H and/or C−H). ^{1}H NMR (DMSO-d_6, δ): 2.97 (s, 12 *H*, N−C*H$_3$*), 2.77 (s, 4 *H*, N−C*H$_2$*). ^{13}C{^{1}H} NMR (DMSO-d_6, δ): 64.29 (N−*C*H$_2$), 53.57 (N−*C*H$_3$).

8·(OTf)$_2$. AgSO$_3$CF$_3$ (0.58 g, 2.23 mmol) was added to a suspension of **7** (0.62 g, 1.10 mmol) in EtCN (4 mL), and the mixture was stirred in the dark at room temperature for 12 h, whereupon it was filtered to remove the solid AgI and the solvent was evaporated to dryness under vacuum to give a pale yellow oily residue. The latter was dissolved in a CH$_2$Cl$_2$−Me$_2$CO solvent mixture (2/1 v/v), and the released solid AgI was centrifugated and separated by decantation. The solution was evaporated under vacuum at 20–25 °C to give a colorless oily residue, which was dried under vacuum at 20–25 °C. The residue was used for further synthetic transformations. ESI$^+$-MS (*m/z*): 439 [M + H$_2$O]$^+$, 384 [M − EtCN + H$_2$O]$^+$. IR (KBr, selected bands, cm^{-1}): 2997 (m-w), 2961 (m-w), ν(C−H from Et); 2187 (w), ν(C≡N); 1266 (vs), 1165 (s), 1032 (s), ν(C−N from the tmeda). ^{1}H NMR (Me$_2$CO-d_6, δ): 3.28 (s, 4 *H*, N−C*H$_2$*), 3.23 (s, 12 *H*, N−C*H$_3$*), 2.96 (q, J_{HH} = 7.3 Hz, 4 *H*, −C*H$_2$*CH$_3$), 1.45 (t, J_{HH} = 7.3 Hz, 6 *H*, −CH$_2$C*H$_3$*). ^{13}C{^{1}H} NMR (Me$_2$CO-d_6, δ): 65.64 (N−*C*H$_2$), 53.72 (N−*C*H$_3$), 13.41 (−*C*H$_2$CH$_3$), 9.48 (−CH$_2$*C*H$_3$).

9·(OTf)$_2$. A solution of the bis(nitrile) complex *cis*-[Pt(tmeda)(EtCN)$_2$][SO$_3$CF$_3$]$_2$ (prepared from *cis*-[PtI$_2$(tmeda)] (1.10 mmol) as described above) in a CH$_2$Cl$_2$−Me$_2$CO solution (2/1 v/v, 2 mL) was treated with an excess of gaseous ammonia for 6 h and stirred at room temperature. The colorless solution was evaporated to dryness under vacuum at 20–25 °C to give a pale yellow oily residue, which was crystallized under a layer of Et$_2$O to furnish the colorless solid. The latter was washed with two 2 mL portions of Et$_2$O (with decantation) and dried under vacuum at 20–25 °C. The yield is 0.70 g, 85%.

Anal. Calcd for PtC$_{14}$H$_{32}$N$_6$F$_6$S$_2$O$_6$: C, 22.31; H, 4.28; N, 11.15. Found C, 22.68; H, 4.31; N, 10.46. FAB$^+$-MS (*m/z*): 381 [M − L − 2H]$^+$, 115 [tmeda − H]$^+$, 72 [L]$^+$. IR (KBr, selected bands, cm^{-1}): 3403 (m), 3338 (m), 3295 (m), 3242 (m), ν(N−H); 2991 (m-w), 2942 (m), ν(C−H from Et); 1659 (s), 1616 (s), ν(C=N);

1229 (s), 1166 (s), 1026 (s), ν(C−N from the amidine or tmeda). ^{1}H NMR (Me$_2$CO-d_6, δ): 7.43 (s, br, 2H, −NH$_2$), 7.07 (s, br, 2H, −NH$_2$), 6.68 (s, br, 2H, −NH=C−), 3.08 (s, 4*H*, N−C*H$_2$*), 2.97 (s, 12*H*, N−C*H$_3$*), 2.51 (q, J_{HH} = 7.3 Hz, 4H, −C*H$_2$*CH$_3$), 1.21 (t, J_{HH} = 7.3 Hz, 6H, −CH$_2$C*H$_3$*). ^{13}C{^{1}H} NMR (Me$_2$CO-d_6, δ): 173.80 (C=N), 64.28 (N−*C*H$_2$), 51.42 (N−*C*H$_3$), 11.89 (−*C*H$_2$CH$_3$). TG curve (Figure S1, Supporting Information): >115 °C gradual dec. When the colorless *cis*-[Pt(tmeda){NH=C-(NH$_2$)Et}$_2$][SO$_3$CF$_3$]$_2$ was heated in the solid phase at 200 °C for 12 h, the complex turned into a dark brown yet unidentified compound, which was characterized by ^{1}H NMR spectroscopy (Me$_2$CO-d_6, δ): 8.48 (s, br, 6H, N*H*), 3.06 (s, 4H, N−C*H$_2$*), 2.99 (s, 12H, NC*H$_3$*), 2.71 (q, J_{HH} = 7.3 Hz, 4H, −C*H$_2$*CH$_3$), 1.36 (t, J_{HH} = 7.3 Hz, 6H, −CH$_2$C*H$_3$*).

cis-[Pt(tmeda){NH=C(NH$_2$)Et}$_2$][C$_6$H$_2$N$_3$O$_7$]$_2$ was obtained by mixing *cis*-[Pt(tmeda){NH=C(NH$_2$)Et}$_2$][SO$_3$CF$_3$]$_2$ with a 2-fold excess of picric acid at room temperature in methanol solution, giving a yellow solution followed by slow evaporation at room temperature to furnish crystals suitable for X-ray crystallography. *Caution!* Picrate salts of metal complexes are potentially explosive!

10·(OTf)$_2$·H$_2$O. HN=C(NHPh)$_2$ (0.06 g, 0.28 mmol) was added to a solution of *cis*-[Pt(tmeda)(EtCN)$_2$][SO$_3$CF$_3$]$_2$ [prepared from *cis*-[PtI$_2$(tmeda)] (0.14 mmol) as described above] in CH$_2$Cl$_2$ (2 mL) and the reaction mixture was stirred for 6 h at room temperature. A lilac residue formed was thoroughly washed (with decantation) with small portions of Et$_2$O and CHCl$_3$ to avoid dissolution of the target product. Yield is 0.05 g, 46%.

Anal. Calcd for PtC$_{14}$H$_{29}$N$_5$F$_6$S$_2$O$_6$·H$_2$O: C, 22.28; H, 4.14; N, 9.28. Found C, 22.57; H, 4.25; N, 9.33. ESI$^+$-MS (*m/z*): 437 [M − H]$^+$. IR (KBr, selected bands, cm^{-1}): 3439 (m), 3269 (m), ν(N−H); 2831 (m-w), ν(C−H from Et); 1610 (s), 1547 (s), ν(C=N); 1224 (s), 1163 (s), 1030 (s), ν(C−N from the 1,3,5-triazapentadiene and/or tmeda). ^{1}H NMR (Me$_2$CO-d_6, δ): 10.94 (s, br, 1H, −NH−), 9.22 (s, br, 2H, −NH=C−), 3.23 (s, 4H, N−C*H$_2$*), 3.17 (s, 12H, N−C*H$_3$*), 2.83 (q, J_{HH} = 7.3 Hz, 4H, −C*H$_2$*CH$_3$), 1.32 (t, J_{HH} = 7.3 Hz, 6H, −CH$_2$C*H$_3$*). ^{13}C{^{1}H} NMR (Me$_2$CO-d_6, δ): 163.81 (C=N), 64.94 (N−*C*H$_2$), 52.26 (N−*C*H$_3$), 11.56 (−*C*H$_2$CH$_3$).

[Pt(tmeda){*N*HC(Et)NHC(Et)*N*H}][C$_6$H$_2$N$_3$O$_7$]$_2$ was obtained by mixing the *cis*-[Pt(tmeda){*N*HC(Et)NHC(Et)*N*H}][SO$_3$CF$_3$]$_2$ complex with a 2-fold excess of picric acid at room temperature in methanol solution, giving a yellow solution followed by its slow evaporation at room temperature to furnish crystals suitable for X-ray crystallography. *Caution!* Picrate salts of metal complexes are potentially explosive!

Attempted Reaction between 10·(OTf)$_2$·H$_2$O and Ammonia. The complex (20 mg) was dissolved in MeOH (2 mL). The obtained solution was stirred under an atmosphere of gaseous ammonia at 20–25 °C for 6 h, whereupon the solvent was evaporated to dryness at room temperature under vacuum, redissolved in Me$_2$CO-d_6, and characterized by ^{1}H NMR spectroscopy. The obtained spectrum corresponds to the intact **10·**(OTf)$_2$, and no traces of **9·**(OTf)$_2$ were detected.

Reaction of *trans*-[PtCl$_2$(RCN)$_2$] and DPG (2 equiv). *trans*-[PtCl$_2$(RCN)$_2$] (R = Et, CH$_2$Ph, Ph) (0.12 mmol) and HN=C(NHPh)$_2$ (50.7 mg, 0.24 mmol) were dissolved in EtCN (1 mL) (R = Et) or CH$_2$Cl$_2$ (1 mL) (R = CH$_2$Ph, Ph) and left to stand for 24 h (R = Et) or 15 h (R = CH$_2$Ph, Ph) at 20–25 °C. The yellow solutions (R = Et, CH$_2$Ph, Ph) were evaporated to dryness. The pale yellow solid residue for R = Et was washed with one 0.5 mL portion of MeOH, filtered off, washed with one 0.5 mL portion of Et$_2$O, and dried in air at 20–25 °C. Products for R = CH$_2$Ph, Ph were separated from yellow oily residues by column chromatography on SiO$_2$ (silica gel 60 F$_{254}$, 0.063–0.200 mm, Merck; eluent

1/10 Et$_2$O−CHCl$_3$ (R = CH$_2$Ph) or 1/20 ethyl acetate−CHCl$_3$ (R = Ph), first fractions) and washed with one 0.5 mL portion of Et$_2$O. Yields are 30 mg, 45% (R = Et), 21 mg, 26% (R = CH$_2$Ph), and 15 mg, 20% (R = Ph).

11. Anal. Calcd for C$_{19}$H$_{22}$N$_5$ClPt: C, 41.42; H, 4.02; N, 12.71. Found: C, 41.89; H, 4.19; N, 12.78. FAB$^+$-MS (*m/z*): 550 [M]$^+$, 515 [M − Cl]$^+$, 495 [M − EtCN]$^+$, 459 [M − HCl − EtCN]$^+$. TLC: R_f = 0.39 (eluent 1/20 Me$_2$CO−CHCl$_3$). IR (KBr, selected bands, cm^{-1}): 3456 (m-w), 3355 (m-w), ν(N−H); 1636 (s), ν(C=N); 1582 (s), 1543 (s), ν(C=N and/or C=C from Ar). ^{1}H NMR (CDCl$_3$, δ): 7.47 (t, 2H), 7.30 (d, 2H), 7.27–7.16 (m, 5H), 6.98 (t, 1H) (Ph), 6.64 (s, br, 1H), 5.87 (s, 1H) (N*H*), 2.33 (q, 7.6 Hz, 2H, C*H$_2$* in N≡C*Et*), 2.16 (q, 7.6 Hz, 2H, C*H$_2$* in HN=C*Et*), 1.19 (t, 7.6 Hz, 3H, C*H$_3$* in N≡C*Et*), 0.94 (t, 7.6 Hz, 3H, C*H$_3$* in HN=C*Et*). ^{13}C{^{1}H} NMR (CDCl$_3$, δ): 164.91 (C=N−H), 148.68, 147.00, 139.87 (C=N−Ph and/or *C*$_{ipso}$), 129.90, 128.66, 128.24, 127.05, 123.47, 122.37 (carbons in Ph), 118.05 (*C*≡N), 33.34 (*CH$_2$* in HN=C*Et*), 12.09 (*CH$_2$* in N≡C*Et*), 11.75 (*CH$_3$* in HN=C*Et*), 9.54 (*CH$_3$* in N≡C*Et*).

12. Anal. Calcd for C$_{29}$H$_{26}$N$_5$ClPt: C, 51.60; H, 3.88; N, 10.37. Found: C, 51.64; H, 3.91; N, 10.38. FAB$^+$-MS (*m/z*): 676 [M + H]$^+$, 640 [M + H − Cl]$^+$, 558 [M − PhCH$_2$CN]$^+$, 522 [M − Cl − PhCH$_2$CN]$^+$. TLC: R_f = 0.64 (eluent 1/10 Et$_2$O−CHCl$_3$). IR (KBr, selected bands, cm^{-1}): 3408 (m-w), 3362 (m-w), 3332 (m-w), ν(N−H); 3055 (w), 3026 (w), ν(C−H from Ar); 2949 (w), 2916 (w), ν(C−H from C*H$_2$*Ph); 1598 (m-s), 1570 (s), ν(C=N and/or C=C from Ar); 746 (m), 698 (m-s), δ(C−H from Ar). ^{1}H NMR (CDCl$_3$, δ): 7.36–7.23 (m, 12H), 7.09 (q, 3H), 7.04–7.01 (m, 4H), 6.96 (t, 1H) (Ph's), 6.76 (s, br, 1H), 5.85 (s, 1H) (N*H*), 3.63 (s, 2H), 3.51 (s, 2H) (C*H$_2$*Ph). ^{13}C{^{1}H} NMR (CDCl$_3$, δ): 162.62 (C=N−H), 148.28, 147.12, 139.67, 136.52 (C=N−Ph and/or *C*$_{ipso}$), 130.09, 129.90, 129.65, 129.00, 128.67, 128.46, 128.01, 127.56, 127.33, 127.05, 123.40, 122.21 (carbons in Ph), 115.56 (*C*≡N), 46.45, 24.39 (*CH$_2$*Ph).

13. Anal. Calcd for C$_{27}$H$_{22}$N$_5$ClPt: C, 50.12; H, 3.43; N, 10.82. Found: C, 50.44; H, 3.35; N, 10.76. FAB$^+$-MS (*m/z*): 647 [M]$^+$, 611 [M − Cl]$^+$, 543 [M − PhCN]$^+$, 507 [M − HCl − PhCN]$^+$. TLC: R_f = 0.69 (eluent 1/20 Me$_2$CO−CHCl$_3$). IR (KBr, selected bands, cm^{-1}): 3396 (m-w), 3366 (m-w), ν(N−H); 3060 (m-w), ν(C−H from Ar); 2274 (w), ν(C≡N); 1594 (s), 1560 (s), 1519 (s), ν(C=N and/or C=C from Ar); 752 (m), 697 (m-s), δ(C−H from Ar). ^{1}H NMR (CDCl$_3$, δ): 7.88 (d, 2H), 7.64 (t, 1H), 7.49–7.36 (m, 12H), 7.30–7.19 (m, 4H), 7.06 (t, 1H) (Ph), 6.50 (s, 1H), 6.00 (s, 1H) (N*H*). ^{13}C{^{1}H} NMR (CDCl$_3$, δ): 158.37 (C=N−H), 148.69, 147.95, 139.84 (C=N−Ph and/or *C*$_{ipso}$), 134.58, 133.29, 130.72, 130.13, 129.40, 128.86, 128.74, 128.17, 127.48, 127.21, 123.96, 123.29 (carbons in Ph), 110.26 (*C*≡N).

Reaction of *trans*-[PtCl$_2$(RCN)$_2$] and DPG (4, 6, or 8 equiv). *trans*-[PtCl$_2$(RCN)$_2$] (R = Et, CH$_2$Ph, Ph) (0.10 mmol) and HN=C(NHPh)$_2$ (85 mg, 0.40 mmol for **4 equiv**, 127 mg, 0.60 mmol for **6 equiv**, and 169 mg, 0.80 mmol for **8 equiv**) were dissolved in the corresponding RCN (1 mL) (R = Et, CH$_2$Ph, Ph) and left to react with stirring for 48 h (R = Et) or without stirring for 24 h (R = CH$_2$Ph, Ph) at 75 °C. The obtained colorless precipitate for R = Et was separated by decantation, washed with two 1.5 mL portions of Me$_2$CO and one 1.5 mL portion of Et$_2$O, and dried in air at 20–25 °C. The solution for R = CH$_2$Ph, Ph was evaporated to dryness, and the colorless (R = CH$_2$Ph) or yellow (R = Ph) needlelike precipitate was washed with one 1 mL portion of Me$_2$CO, filtered off, washed with one 1 mL portion of Me$_2$CO and one 1 mL portion of Et$_2$O, and dried in air at 20−25 °C. TG curves: 277 and 282 °C (for complexes **14** and **15**, respectively) and 301 °C (for complex **16**). Yields of complexes do not depend significantly on the amount of DPG (4, 6, or 8 equiv). Yields are 46 mg, 63% (R = Et), 62 mg, 73% (R = CH$_2$Ph), and 55 mg, 67% (R = Ph) (data for reactions performed with *trans*-[PtCl$_2$(RCN)$_2$] and 4 equiv of DPG).

14. Anal. Calcd for C$_{32}$H$_{34}$N$_8$Pt: C, 53.00; H, 4.70; N, 15.41. Found: C, 53.61; H, 4.87; N, 15.65. FAB$^+$-MS (*m/z*): 726 [M]$^+$. TLC: R_f = 0.53 (eluent 1/4 Me$_2$CO−CHCl$_3$). DTA/TG: 277 °C (gradual dec). IR (KBr, selected bands, cm^{-1}): 3420 (m-s), 3355 (m-s), ν(N−H); 3093 (w), 3057 (m-w), 3023 (m-w), ν(C−H from Ar); 2962 (m), 2935 (m-w), 2908 (m-w), 2875 (m-w), 2825 (w), 2779 (w), ν(C−H from Et); 1596 (s), 1571 (s), 1538 (m-s), ν(C=N and/or C=C from Ar); 749 (m-s), 702 (s), δ(C−H from Ar). ^{1}H NMR (CDCl$_3$, δ): 7.56 (t, 4H), 7.38–7.28 (m, 6H), 7.21–7.12 (m, 8H), 6.93 (t, 2H) (Ph), 5.81 (s, br, 2H), 4.88 (s, br, 2H) (N*H*), 1.92 (q, 7.5 Hz, 4H), and 0.71 (t, 7.5 Hz, 6H) (*Et*). ^{13}C{^{1}H} NMR (CDCl$_3$, δ): 165.04 (C=N−H), 147.64, 144.91, 140.55 (C=N−Ph and/or *C*$_{ipso}$), 130.83, 128.83, 128.58, 127.26, 122.80, 121.89 (carbons in Ph), 33.68 (*CH$_2$*), and 10.50 (*CH$_3$*) (*Et*).

15. Anal. Calcd for C$_{42}$H$_{38}$N$_8$Pt: C, 59.36; H, 4.51; N, 13.18. Found: C, 59.59; H, 4.55; N, 13.55. FAB$^+$-MS (*m/z*): 849 [M]$^+$. TLC: R_f = 0.45 (eluent 1/10 Et$_2$O−CHCl$_3$). DTA/TG: 282 °C (gradual dec). IR (KBr, selected bands, cm^{-1}): 3413 (m-s), 3338 (m-s), ν(N−H); 3057 (m-w), 3029 (m-w), ν(C−H from Ar); 2954 (w), 2928 (w), ν(C−H from *CH$_2$*Ph); 1602 (s), 1572 (s), 1538 (m-s), ν(C=N and/or C=C from Ar); 749 (m-s), 702 (s), δ(C−H from Ar). ^{1}H NMR (CDCl$_3$, δ): 7.43 (t, 4H), 7.27–7.20 (m, 11H), 7.11–6.99 (m, 13H), 6.91 (t, 2H) (Ph), 5.75 (s, br, 2H), 4.81 (s, br, 2H) (N*H*), 3.12 (s, 4H, C*H$_2$*Ph). The compound is poorly soluble in all common deuterated solvents, and this precluded ^{13}C{^{1}H} NMR measurements.

16. Anal. Calcd for C$_{40}$H$_{34}$N$_8$Pt: C, 58.46; H, 4.17; N, 13.63. Found: C, 58.12; H, 4.17; N, 13.12%. FAB$^+$-MS (*m/z*): 822 [M + H]$^+$. TLC: R_f = 0.41 (eluent 1/20 Et$_2$O−CHCl$_3$). DTA/TG: 302 °C (gradual dec). IR (KBr, selected bands, cm^{-1}): 3422 (m), 3366 (m), ν(N−H); 3057 (m-w), ν(C−H from Ar); 1590 (m-s), 1558 (s), 1522 (m-s), ν(C=N and/or C=C from Ar); 749 (m), 694 (m-s), δ(C−H from Ar). ^{1}H NMR (CDCl$_3$, δ): 7.65 (t, 4H), 7.45 (d, 6H), 7.35 (t, 2H), 7.24–7.13 (m, 16H), 7.01 (t, 2H) (Ph), 5.91 (s, 2H), 5.68 (s, br, 2H) (N*H*). The compound is poorly soluble in all common deuterated solvents, and this precluded ^{13}C{^{1}H} NMR measurements.

Supporting Information Available: Figure S1, giving the TG curve for **9**·(OTf)$_2$, Figures S2–S4, giving molecular structures of **1**, **2**, and **11**, Figure S5, giving the hydrogen-bonding scheme for **4**, Table S1, giving the hydrogen bonds for **4**, CIF files giving crystallographic data, and text giving a detailed description of the synthetic procedure for *cis*-[PtI$_2$(tmeda)] (**7**). This material is available free of charge via the Internet at http://pubs.acs.org.

IC702483W